AD NUMBER
AD015448
CLASSIFICATION CHANGES
TO: unclassified
FROM: confidential
LIMITATION CHANGES
TO: Approved for public release, distribution unlimited
FROM: Distribution authorized to U.S. Gov't. agencies and their contractors; Administrative/Operational Use; JUN 1953. Other requests shall be referred to Chief of Naval Operations, Washington, DC.
AUTHORITY
30 Jun 1965, DoDD 5200.10; DTMB ltr 23 Feb 1966

AD _____

AD-

154488

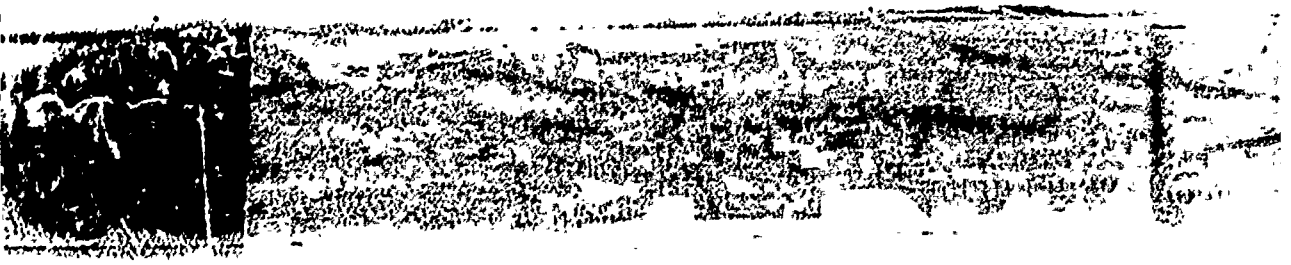

NAVY DEPARTMENT
THE DAVID W. TAYLOR MODEL BASIN
WASHINGTON 7, D.C.

THEORETICAL CONSIDERATIONS ON SHROUDED PROPELLERS

by
H. W. Lerbs, Dr. Ing.

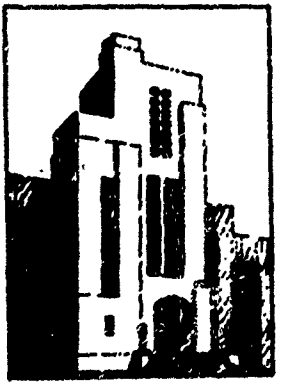

6

June 1953 Report C-543

THEORETICAL CONSIDERATIONS ON SHROUDED PROPELLERS

by

H.W. Lerbs, Dr. Ing.

June 1953

Report C-543

TABLE OF CONTENTS

NOTATION

P	Power input
T	Thrust
Q	Tangential force
n	Number of blades
$D = 2R$	Diameter (of rotor and shroud)
l	Length of shroud
$h = l/2R$	Length-diameter ratio of shroud
r_h	Hub radius
r, a, ϕ	Cylindrical coordinates
$x = r/R$, $z = \frac{a}{l/2}$	Nondimensional cylindrical coordinates
v_0	Velocity of approach
ω	Angular velocity
$\lambda = v_0/\omega R$	Advance coefficient
Γ	Circulation
$G = \frac{\Gamma}{v_0 D}$	Nondimensional circulation
w_a	Axial component of induced velocity
w_r	Radial component of induced velocity
w_t	Tangential component of induced velocity
e	Sink density per unit area
σ	Cavitation number
c_D	Drag coefficient
c_L	Lift coefficient

$\epsilon = c_D/c_L$	Drag-lift ratio
$c_T = \dfrac{T}{\frac{\rho}{2}(R^2 - r_h^2)\,\pi v_0^2}$	Thrust coefficient
$c_P = \dfrac{P}{\frac{\rho}{2}(R^2 - r_h^2)\,\pi v_0^3}$	Power coefficient
F, E, K, P_n, I, S, i_t	Symbols for functions which are defined in the paper

ABSTRACT

The flow and the forces which are generated by a propulsion system consisting of rotor, shroud and guide vanes are analyzed. For this purpose, the components of the system are replaced by proper singularities. From the component velocity fields and from the characteristic constants of the singularities, the interaction forces between the components are determined from which the net forces of the unit follow. The deduced expressions for thrust and power input taken together with the pressure increase at the rotor, which arises from the action of the shroud, and with the condition of cavitation free flow form the basis for a method of design of a propulsion unit. To apply this method, knowledge of both lift versus angle of attack curves and of pressure distribution curves of sections in cascade is necessary.

Comparison of experimental results for the efficiency and for the interaction force between rotor and shroud are in fair agreement with the respective analytical expressions taking into account the lack of knowledge relative to the drag of the shroud.

1. INTRODUCTION

Recent interest by the U.S. Navy in the possible application of shrouded propellers to various types of naval vessels for the purpose of delaying cavitation and propeller noise has led to a study of the available theory of such a propulsion system. It was found desirable to consider further the theoretical aspects of this problem which has resulted in the development of the theory represented here. It is planned to supplement this work with a presentation of the theory as applied to a specific design problem.

The forces on the components of the system and the design data are to be determined for a given net thrust of a propulsion system consisting of rotor, shroud, and guide vanes (the latter two components being stationary) and for given quantities of speed of advance, number of revolutions, rotor diameter, and pressure at the rotor (due to the action of the shroud). For this problem, it is necessary to ascertain the mutual interaction between the components of the system which follows when these components, with respect to their effect on the flow, are replaced by proper singularities. In order to deduce the component forces on the basis of such a theory, it is necessary to know the component velocity fields. This requires certain approximations which will be mentioned first in connection with the singularities.

The shroud is considered to be an annular-shaped thin hydrofoil; all the sections, determined by a meridian cut, are supposed to be of equal shape. This axisymmetrical hydrofoil is replaced by a row of adjacent circular vortices. Furthermore, it is assumed that the shroud is a circular cylinder with a diameter equal to that of the rotor. This approximation

holds if both the ordinates of the camber line of the hydrofoil section as measured from the cylinder and the square of the slope of the ordinates are small. Then, the circular vortices can be arranged on the surface of the cylinder, i.e., their diameter is constant and equals that of the rotor.

The gap between rotor and shroud is assumed to be very small and the length of the shroud to be sufficiently great so that a radial flow around the tips of the rotor blades and the equalizing of pressure which arises from such radial flow are prevented. Then a circulation which is independent of the radius is possible at the rotor for which free vortices are not present. When the blades are replaced by lifting lines, the vortex system of the rotor then consists merely of the lifting lines and of a hub vortex of the combined circulation of that of the lifting lines. Further, discontinuities of the velocity components occur within the boundary of the rear part of the jet. The introduction of helical vortex lines within the boundary would be necessary to account for these discontinuities.

With respect to the velocity field of the rotor, the influence of a finite number of blades is neglected; by this simplification, the field of the absolute velocity becomes independent of time. It is shown later that this assumption may be justified with the number of blades in practical application. Then the discontinuity of the velocity within the boundary of the rear jet is equivalent to a vortex sheet consisting of helical vortex lines. It is well known that such a sheet can be resolved into two sheets, one consisting of straight vortex lines which are parallel to the axis and the other one of ring vortices which are perpendicular to the axis.

The first sheet produces only tangential velocity components, as follows from the law of Biot-Savart. Within the inside fluid, i.e., within the slipstream, the velocity from this sheet equals zero (as follows from Stokes' law). The tangential velocity components produced from this sheet on the shroud (which is within the outside fluid) are without interest for the interaction between rotor and shroud. Hence, the sheet consisting of straight vortex lines need not be considered in the following.

The sheet of ring vortices can be replaced by singularities on the propeller disk. It is well known that the velocity potential of a single closed vortex equals that of a uniform distribution of dipoles over any surface bounded by the vortex, the axes of the dipoles being perpendicular to the surface (e.g., see Lamb, Hydrodynamics, Art. 150, 161, and 102). The singularities on the disk which correspond to a row of closely adjacent ring vortices behind the disk follow when integrating the potential of a single ring vortex from $z = 0$ (at the rotor disk) to infinity downstream, as given in Lamb, Art. 161 (13). The result for the inflow is that the potential of this row of ring vortices equals that of a uniform sink distribution over the disk. The same result has been obtained by Dickman in a different way, viz., from Euler's differential equations.[1]

References are listed on page 43.

In the following discussion, the rotor inflow is based on the flow of a sink disk by which numerical calculations become simpler than from the velocity field of the cylindrical vortex sheet at the boundary of the rear jet. The force on the rotor, however, is not calculated from the forces which act on the sinks but from those on the lifting vortices, permitting the influence of a finite number of blades on the force to be approximated.

Analagously, the guide vanes are replaced by lifting lines in order to determine the forces. The total circulation of these lifting lines is taken equal to that of the rotor in which case, with a finite number of blades, the average of the tangential velocity component within the slipstream equals zero at the design advance coefficient. With respect to the influence of the guide vanes on the axial and radial inflow, which depends on the thrust loading, rotor and vanes are considered as a unit which causes the sum of the component thrusts. Correspondingly, the strength of the sinks at the rotor disk is determined from the sum of the thrusts of rotor and vanes. This amounts to a neglect of both the finite distance between rotor and vanes and of the variation of the circulation with time which arises from the interference between rotor and vanes with a finite number of blades.

The vanes are considered to be situated behind the rotor. In this position, the vanes cause a thrust which is in the same direction as the thrust generated by the rotor. On the other hand, due to the pressure increase which arises from the positive thrust, the losses at the vanes are greater than when located in front of the rotor. In this latter arrangement, a negative thrust arises at the vanes which leads to a pressure drop and, therefore, to small losses. At the same time, the necessary lift coefficients at the rotor are smaller in the latter arrangement because of a greater relative velocity; this advantage with respect to the onset of cavitation may be offset by the smaller cavitation numbers of the sections of the rotor.

The termination of the rotor shaft requires singularities which are chosen so that the meridian cut of the shaft becomes a streamline of the combined flow. If this condition is not satisfied, the continuity equation is violated. Approximately, however, a single sink on the axis may be sufficient to account for the effect of the shaft.

When the components of the system are replaced by the afore-mentioned singularities within a uniform velocity field, which is identical with the speed of advance, the force acting on any one singularity follows from a general rule (Lagally). For the problem under consideration, the main consequence of this general rule is that the interference velocity on each of the singularities arising from the other singularities present does not lead to a resultant force but to interaction forces between the singularities. From this, the reaction between shroud and rotor, e.g., is determined either from the singularities of the shroud and the velocity induced at the shroud from the rotor or from the singularities of the rotor and the velocity induced at the rotor from the shroud. The force follows from the product of the characteristic constant of the singularity (e or Γ) times the velocity. In the case of a sink singularity, the direction of the force equals that of the velocity; in the case of a vortex,

the force is normal to the velocity and coincides with the vector product ($v \times \text{curl } v$). This latter special case of the general rule is the well-known law of Kutta-Joukowsky.

2. THE VELOCITY FIELDS

2.1 THE VELOCITY FIELD OF THE SHROUD

The velocity field of the shroud is determined from its chordwise circulation distribution; two cases can be considered in this respect, viz., the shape of the shroud is given and the circulation distribution is to be determined or vice versa. In both of these cases, the unknown quantity follows from the boundary condition of the flow, viz., that the section of the shroud is a streamline of the relative flow at the shroud. This flow results from the undisturbed flow, from the induction of rotor, guide vanes, and shaft sink, and from the self-induction of the shroud.

The problem of determining the circulation distribution, neglecting the thickness of the shroud section and considering the camber line given, leads to a complicated integral equation for which Dickmann gives an approximate solution.[2] However, this solution becomes very laborious when $h = l/2R \geq 1$, h being the ratio of shroud length to its diameter. This case cannot be excluded from consideration. Therefore, it is desirable to avoid beginning with a given camber line and to begin instead with a given circulation distribution which necessitates the determination of the camber line afterwards such that the circulation distribution is realized, i.e., that the afore-mentioned boundary condition of the resultant flow is satisfied. Proceeding in this way avoids the integral equation, and the camber line follows from a first-order differential equation.

The circulation function over the chord length of the shroud is chosen to be a half ellipse in order to avoid peaks of negative pressure. This circulation function requires that the forward stagnation point be situated at the leading edge of the camber line (shock-free condition). It is well known that this condition is satisfied in the case of two-dimensional flow at a flat wing with a parabolic camber line at zero angle of attack. The camber line and the geometric angle of attack of a ring-shaped wing which satisfy the shock-free condition are not yet known. Both of these unknowns can be determined after the component velocity fields have been established.

For the velocity field of the shroud, a cylindrical sheet of adjacent circular vortices is considered corresponding to the afore-mentioned assumptions. The stream function of a single circular vortex of radius R, width da', and circulation $(\gamma da')$ is, in cylindrical coordinates, r, a, and φ, represented by (e.g., see Lamb, Art. 161)

$$d\underline{\psi} = -\frac{1}{2\pi}(\gamma da')(rR)^{\frac{1}{2}}\, k(2D-K) \quad with \quad D=\frac{K-E}{k^2}$$

K and E are the complete elliptic integrals of the first and second kind, respectively, of modulus k which is determined by

$$k^2 = \frac{4rR}{(a-a')^2+(r+R)^2}$$

where a' fixes the location of the vortex ring.

From this expression for the stream function, the velocity components of a single circular vortex ring are deduced when applying the following relations for the derivatives of the complete elliptic integrals with respect to the modulus

$$\frac{d(kD)}{dk} = -\frac{d^2E}{dk^2} = \frac{K-D}{1-k^2}$$

$$\frac{d(kK)}{dk} = \frac{E}{1-k^2}$$

One obtains

$$dw_a = -\frac{\gamma da'}{\pi} \frac{R}{[(a-a')^2+(r+R)^2]^{\frac{3}{2}}} \left\{ 2rD + (R-r)\frac{E}{1-k^2} \right\}$$

$$dw_r = -\frac{\gamma da'}{\pi} \frac{R(a-a')}{[(a-a')^2+(r+R)^2]^{\frac{3}{2}}} \left\{ \frac{E}{1-k^2} - 2D \right\}$$

$$dw_t = 0$$

Because of the axial symmetry of the problem, both the axial and radial components are independent of the angular coordinate, and, further, the tangential component equals zero.

For a vortex cylinder of any circulation distribution, the velocity components follow from the elementary components of a vortex ring by integration. The result written nondimensionally for an elliptic distribution is:

$$\frac{w_a}{v_o}\frac{1}{G_S} = -\frac{1}{2\pi^2}\int_{-1}^{+1} x^{-\frac{3}{2}}\sqrt{1-z'^2}\; k^3\left\{(1-x)\frac{E(k)}{(k')^2} + 2xD(k)\right\}dz' \qquad [1]$$

$$\frac{w_r}{v_o}\frac{1}{G_S} = \frac{h}{2\pi^2}\int_{-1}^{+1} x^{-\frac{3}{2}}(z'-z)\sqrt{1-z'^2}\; k^3\left\{\frac{E(k)}{(k')^2} - 2D(k)\right\}dz' \qquad [2]$$

where $\left.\begin{matrix} x = \frac{r}{R} \\ z = \frac{a}{\frac{l}{2}} \end{matrix}\right\}$ are nondimensional cylindrical coordinates,

l is the length of the shroud,

k^2 is $\dfrac{4x}{\left[h(z-z')\right]^2 + (1+x)^2}$

$(k')^2$ is $1 - k^2$,

$h = \dfrac{l}{2R}$ is the ratio of length to diameter of the shroud,

$z' = \dfrac{a'}{l/2}$ is the variable of integration over the chord length of the shroud, and

$G_S = \dfrac{\Gamma_S}{(2R v_0)}$ is the nondimensional total circulation of the shroud. This quantity is positive if the force which is generated by a positive v_0 (in the direction of positive a) is positive (in the direction of positive r).

The complete elliptic integrals within the velocity components have been expressed by integrals over a product of the modified first order Bessel functions in a paper by Stewart.[3] For numerical purposes, however, the velocity components as written in Equations [1] and [2] are found to be more convenient.

Relative to the problem under consideration, the velocity components of interest are those within the plane normal to the axis through the halfway point of the shroud length, $z = 0$, (in which plane rotor and vanes are supposed to be situated) and, further, at the vortex sheet, $x = 1$.

For the plane $z = 0$, there is obtained from Equations [1] and [2]:

$$\left(\frac{w_a}{v_0}\frac{1}{G_S}\right)_{z=0} = -\frac{1}{\pi^2}\int_0^1 x^{-\frac{3}{2}}\sqrt{1-z'^2}\;k^3\left\{(1-z)\frac{E(k)}{(k')^2} + 2xD(k)\right\}dz'$$

$$\left(\frac{w_r}{v_0}\frac{1}{G_S}\right)_{z=0} = \frac{h}{2\pi^2}\int_{-1}^{+1} x^{-\frac{3}{2}}\,z'\sqrt{1-z'^2}\;k^3\left\{\frac{E(k)}{(k')^2} - 2D(k)\right\}dz' = 0$$

$$k^2 = \frac{4x}{(hz')^2 + (1+x)^2}$$

The radial component in this plane becomes zero since the integrand is an odd function of z'.

At the axis, $x = 0$, the integrand for w_a can be expressed by known functions. One obtains

$$\left(\frac{w_a}{v_0}\frac{1}{G_S}\right)_{\substack{z=0\\x=0}} = -\frac{8}{\pi^2}E(0)\int_0^1 \frac{\sqrt{1-z'^2}\,dz'}{\left[(hz')^2+1\right]^{\frac{3}{2}}} = -\frac{4}{\pi}\frac{k^*}{h^3}\left[(1+h^2)E(k^*)-K(k^*)\right]$$

$$k^* = \frac{h}{\sqrt{1+h^2}}$$

At stations x which are different from zero, the integral for w_a can only be evaluated by numerical calculations. The results of these calculations over a range of h are represented on Figure 2. From this figure it follows that the velocity distribution within the middle plane becomes uniform for shrouds of a length greater than about twice the diameter. For shorter shrouds, the axial velocity becomes increasingly less uniform the shorter the shroud is, the velocity increasing from the axis towards the wall of the shroud.

It should be mentioned that different notations for the same velocity component are used in this report. For instance, the afore-deduced velocity component $(w_a)_{z=0}$ is the

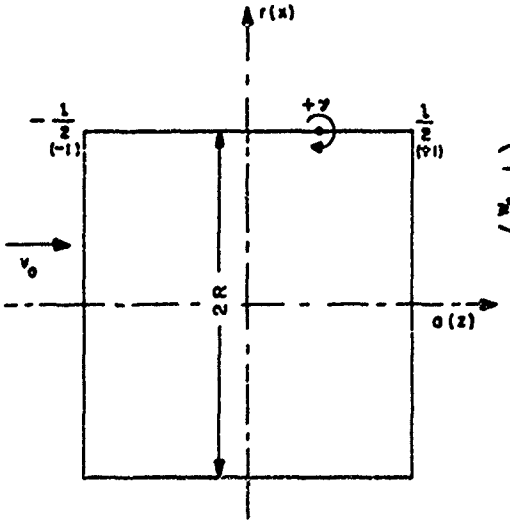

Figure 1

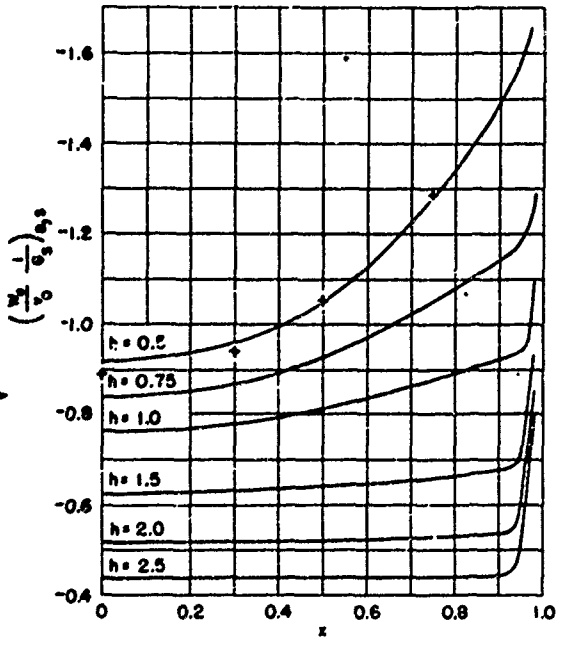

Figure 2 - Velocity Field of the Shroud in the Plane $z = 0$

Middle plane normal to the axis.

component induced at the plane $z = 0$, i.e., at the disk from the shroud. In the application of this work, a notation with two indices is found more convenient. The first index fixing the plane of reference and the second one the component of the system by which the respective velocity component is generated. Correspondingly, the velocity component $(w_a)_{z=0}$ is denoted on the diagrams and later on in this report by $(w_a)_{D,S}$ Analogously, $(w_a)_{S,S}$ denotes the self-induction of the shroud, $(w_a)_{S,D}$ the axial component induced at the shroud from the disk, and so on.

The self-induction of the shroud follows from Equations [1] and [2] with $x = 1$

$$\left(\frac{w_a}{v_0}\frac{1}{G_S}\right)_{x=1} = -\frac{1}{\pi^2}\int_{-(1+z)}^{1-z}\sqrt{1-z'^2}\;k^3 D(k)\,d(z'-z)$$

$$\left(\frac{w_r}{v_0}\frac{1}{G_S}\right)_{x=1} = \frac{h}{2\pi^2}\int_{-1}^{+1}(z'-z)\sqrt{1-z'^2}\;k^3\left\{\frac{E(k)}{(k')^2} - 2D(k)\right\}dz'$$

$$k^2 = \frac{4}{\left[h(z-z')\right]^2+4}$$

Both of these integrals become improper integrals when z' approaches z. In this case, k approaches 1, k' approaches zero, and K approaches infinity as nat log $[1/(z-z')]$. With respect to the integral for w_a, the transformation $(z'-z) = t^n$ is introduced. Then the product $(K\,t^{n-1})$ approaches zero when z' approaches z provided that $n > 1$.

Correspondingly, $n = 3$ is chosen for the numerical evaluation of the integral in order to have real values of t for negative quantities $(z'-z)$; it follows that

$$\left(\frac{w_a}{v_0}\;\frac{1}{G_S}\right)_{x=1} = -\frac{3}{\pi^2}\int_{-\sqrt[3]{1+z}}^{\sqrt[3]{1-z}}\sqrt{1-z'^2}\,k^3 D(k)\,t^2\,dt$$

The results of the numerical evaluation are represented in Figure 8. The curves are symmetrical about $z = 0$.

Relative to w_r, the integral

$$H = \int_{-1}^{+1}(z'-z)\sqrt{1-z'^2}\;k^3\,\frac{E'(k)}{(k')^2}\,dz'$$

is considered first; the integrand becomes indefinite of form 0/0 when z' approaches z. Replacing $(k')^2$ by $(1-k^2)$ gives

$$H = \frac{4}{h^2}\int_{-1}^{+1}\frac{\sqrt{1-z'^2}\;k^3 E}{z'-z}\,dz' + \int_{-1}^{+1}(z'-z)\sqrt{1-z'^2}\;k^3 E\,dz'$$

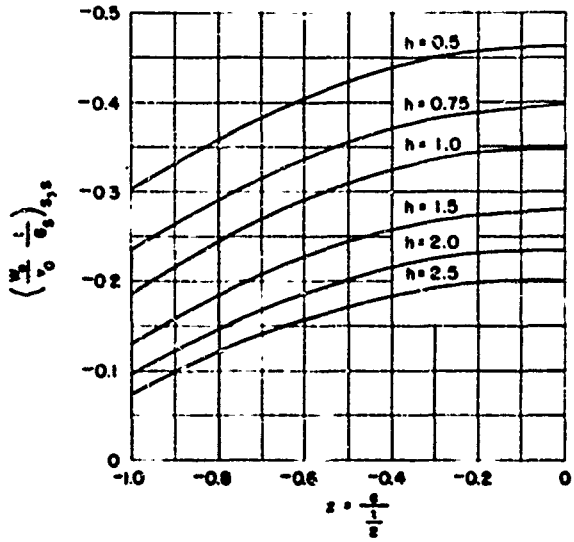

Figure 3 - Self-Induction of the Shroud

Axial Component

The first of these two integrals is an improper integral. To determine its principal value, we introduce $z' = \cos\varphi'$, $dz' = -\sin\varphi' d\varphi'$, $z = \cos\varphi$ and resolve the numerator $(\sqrt{1-z'^2}\,E\,k^3\sin\varphi')$ within the interval, $\varphi' = \pi$ to $\varphi' = 0$, which corresponds to the interval $z = -1$ to $z = +1$, into a Fourier-series

$$\sqrt{1-z'^2}\;k^3E\sin\varphi' = k^3E\sin^2\varphi' = \sum_{n=0}^{\infty} a_n\cos n\varphi'$$

Then it follows that

$$\int_{-1}^{+1}\frac{\sqrt{1-z'^2}\;k^3E}{z'-z}\,dz' = \sum_{n=0}^{\infty} a_n\int_0^{\pi}\frac{\cos n\varphi'}{\cos\varphi'-\cos\varphi}\,d\varphi' = \sum_{n=0}^{\infty} a_n\pi\,\frac{\sin n\varphi}{\sin\varphi} = \frac{\pi}{\sin\varphi}\sum_{n=0}^{\infty} a_n\sin n\varphi$$

With this expression, there is obtained

$$\left(\frac{w_r}{v_0}\,\frac{1}{G_s}\right)_{z=1} = \frac{h}{2\pi^2}\left\{\frac{4}{h^2}\,\frac{\pi}{\sin\varphi}\sum_{n=0}^{\infty} a_n\sin n\varphi + \int_{-1}^{+1}(z'-z)\sqrt{1-z'^2}\;k\left[(2+k^2)E-2K\right]dz'\right\}$$

Within the integral, the product $K(z'-z)$ approaches zero when z' approaches z; thus the integral can be evaluated numerically without difficulty. Relative to the first term within the brackets, this term becomes indefinite of form 0/0 at the end points of the interval $z = -1$ and $z = +1$. From l'Hospital's rule it follows that

$$\text{for } z = -1: \quad \left(\frac{w_r}{v_0}\frac{1}{G_S}\right)_{z=1} = \frac{h}{2\pi^2}\left\{\frac{4}{h^2}\sum_{n=1}^{\infty}(-1)^{n+1} n a_n + \int_{-1}^{+1} \ldots dz'\right\}$$

$$\text{for } z = +1: \quad \left(\frac{w_r}{v_0}\frac{1}{G_S}\right)_{z=1} = \frac{h}{2\pi^2}\left\{\frac{4}{h^2}\sum_{n=1}^{\infty} n a_n + \int_{-1}^{+1} \ldots dz'\right\}$$

The numerical results as obtained by means of Fourier-expansions consisting of six terms a_n are represented on Figure 4. Since the radial component is an odd function of z, it is represented only for an interval of z from -1 to 0.

It should be mentioned that the main difference between a ring-shaped and a flat wing lies in the axial component of the self-induced flow. This component is zero in the case of a flat wing and arises from the lateral parts of the ring for a ring-shaped wing.

The velocity which is induced at the shaft sink from the shroud is determined approximately by assuming the total circulation of the shroud Γ_s concentrated in a single vortex at $z = 0$. From the stream function of a single circular vortex, one obtains at the shaft sink with coordinates $x_{sh} = 0$ and $z_{sh} = a_{sh}/(l/2)$

$$\left(\frac{w_a}{v_0}\frac{1}{G_S}\right)_{sh,S} = -\frac{1}{\left(1 + z_{sh}^2 h^2\right)^{\frac{3}{2}}} \qquad [1a]$$

2.2 THE VELOCITY FIELD OF ROTOR AND GUIDE VANES

As mentioned previously, the effect of rotor and guide vanes on the inflow is deduced from that of an axisymmetrical sink distribution over the rotor disk. For a disk of small thickness δ, the volume element amounts to $dV = r'(dr')(d\varphi)\delta$.

Let q be the strength of the sinks per unit volume; then the strength of the volume element becomes $de = r'(dr')(d\varphi)(q\delta)$. Passing to the limit $\delta = 0$ in such a way that the "surface density" $e_D = q\delta$ remains constant, the elementary strength of the surface element $dA = r'(dr')(d\varphi)$ becomes $(e_D\, dA)$ and induces, at a point with cylindrical coordinates $(a, r, 0)$, the velocity element

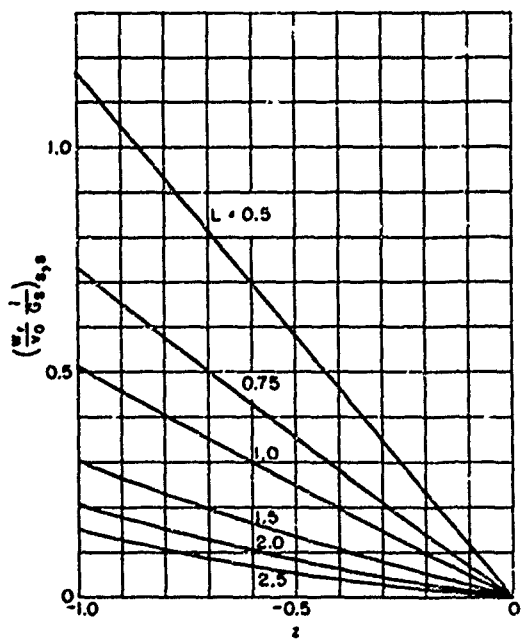

Figure 4 - Self-Induction of the Shroud

Radial Component

$$(d^2w) = \frac{e_D\,dA}{4\pi p^2} = \frac{e_D}{4\pi p^2}\, r'dr'd\varphi$$

where p is the distance between the area element of the disk and the point of reference. If the area element has coordinates $(0, r', \varphi)$, it follows that

$$p^2 = a^2 + (r'\sin\varphi)^2 + (r - r'\cos\varphi)^2$$

For the components of (d^2w), there is obtained:

$$(d^2w)_a = (d^2w)\,\frac{a}{p}$$

$$(d^2w)_r = (d^2w)\cos(r', p) = (d^2w)\left(\frac{r'}{p} - \frac{r}{p}\cos\varphi\right)$$

Introduction of the expressions for (d^2w) and p into these relations and integration over φ yield the following result for the velocity field of an annular sink ring, e_D being independent of φ

$$dw_a = \frac{e_D}{2\pi x'}\,dx'\,\frac{2(hz)(x')^2}{(hz)^2 + (x'-x)^2}\,\frac{E(k)}{\sqrt{(hz)^2 + (x'+x)^2}} = \frac{e_D}{2\pi x'}\,dx'\,w_a^* \qquad [3]$$

$$dw_r = -\frac{e_D}{2\pi x'}\,dx'\,\frac{x'}{\sqrt{(hz)^2 + (x'+x)^2}}$$
$$\left\{K(k) - E(k)\left[1 - \frac{2x'(x'-x)}{(hz)^2 + (x'-x)^2}\right]\right\} = \frac{e_D}{2\pi x'}\,dx'\,w_r^* \qquad [4]$$

The modulus k of the complete elliptic integrals has the value

$$k = \frac{2\sqrt{xx'}}{\sqrt{(hz)^2 + (x'+x)^2}}$$

The tangential component is zero because of axial symmetry.

From these expressions, the velocity components of a sink disk follow when integrating over x'. Since e_D may depend on x', there is obtained

$$w_a = \frac{1}{2\pi}\int_{x_h}^{1} e_D\,\frac{w_a^*}{x'}\,dx' \qquad [3a]$$

$$w_r = -\frac{1}{2\pi}\int_{x_h}^{1} e_D\,\frac{w_r^*}{x'}\,dx' \qquad [4a]$$

where the nondimensional radius of the hub r_h/R is denoted by x_h.

Putting $x = 1$ in the expressions for w_a^* and w_r^* gives the velocity components which

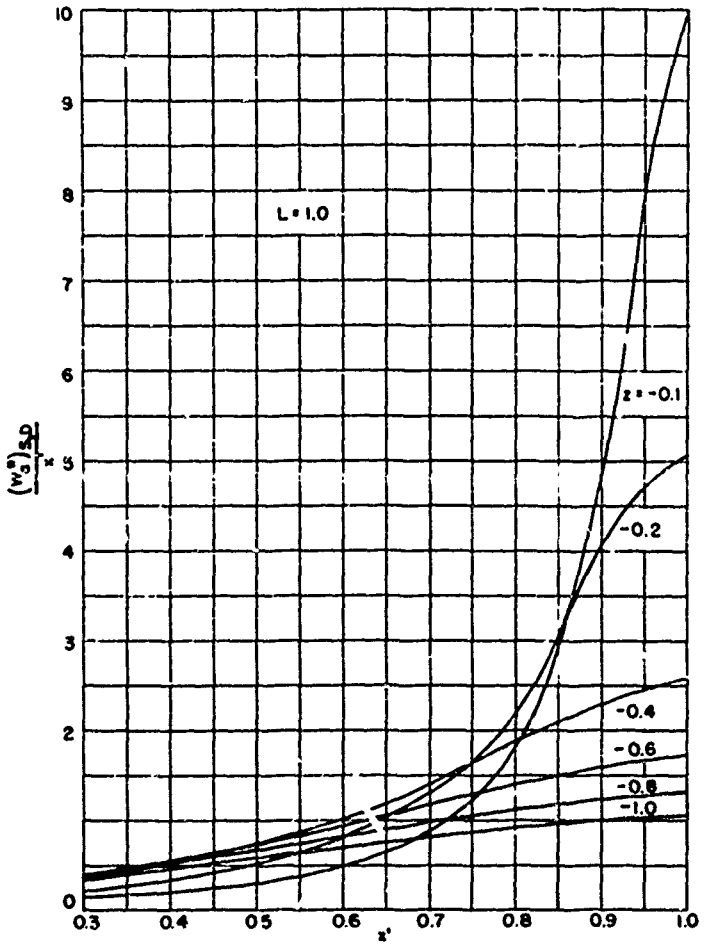

Figure 5

are induced at the shroud from the disk. For this case and for $h = 1.0$, the one factor of the integrands, viz., $(w_a^*/x')_{S,D}$ and $(w_r^*/x')_{S,D}$ is represented on Figures 5 and 6, respectively. In these representations, most of the numerical values of the functions w_a^* and w_r^* have been taken from a paper by Kuechemann.[4] With respect to the influence of h, the determination of the curves for one value of h is sufficient since w_a^* and w_r^*, from Equations [3] and [4], respectively, depend merely on the product $(h\,z)$. That is, for different values of h, the curves for w_a^* and w_r^* shift so that the same ordinate belongs to a different abscissa, which follows from $(h\,z) = \text{constant}$.

In order to determine $(w_a)_{S,D}$ and $(w_r)_{S,D}$, the variation of e_D over the radius must be known. If e_D is independent of x or can be replaced by a suitable average e_D, the expressions become

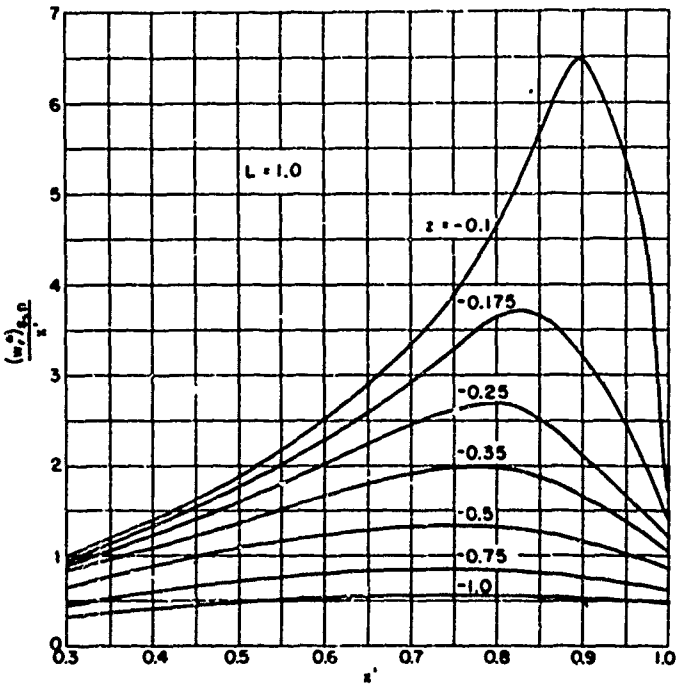

Figure 6

$$(w_a)_{s,l}\,\frac{2\pi}{\bar{e}_l} = \int_{x_h}^{1} \frac{w_a^*}{x'}\,dx' \qquad [3b]$$

$$(w_r)_{s,l}\,\frac{2\pi}{\bar{e}_l} = -\int_{x_h}^{1} \frac{w_r^*}{x'}\,dx' \qquad [4b]$$

which can be computed numerically from the quantities on Figures 5 and 6; the result is given in Figures 7 and 8, respectively, for a hub radius $x_h = 0.4$ and for a range of h. With respect to this latter variable, the curves are related in the same manner as the integrands.

Relative to the self-induction of the sink disk, the axial component of the induced velocity is of interest because of its relation to the thrust. From Equation [3], the component would follow at each station x from:

$$(w_a)_{z=0} = \lim_{z \to 0} \int_{x_h}^{1} dw_a$$

Instead of determining this limit of the integral, there is a more convenient way of ascertaining $(w_a)_{z=0}$ by representing w_a by a series of Legendre polynomials

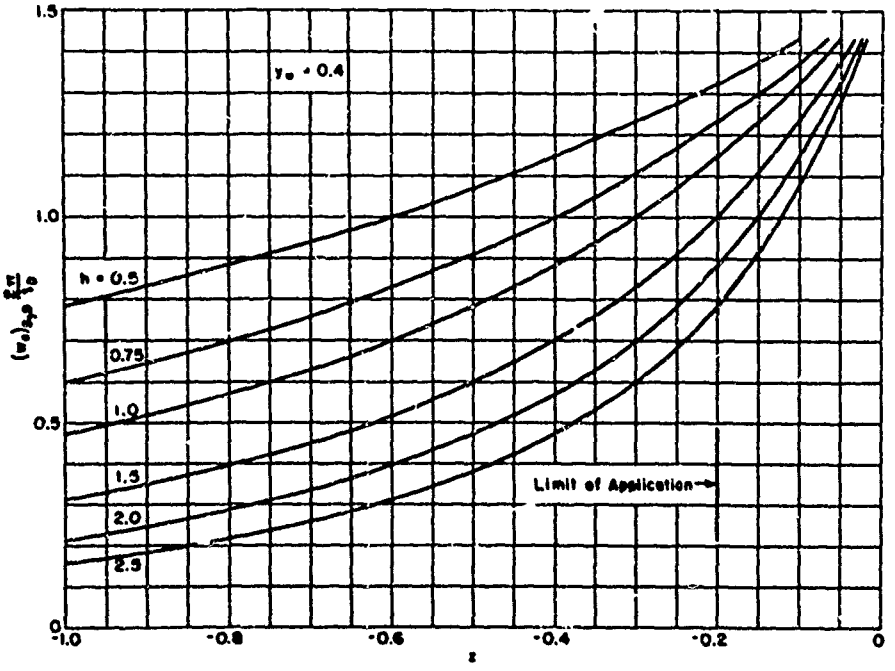

Figure 7

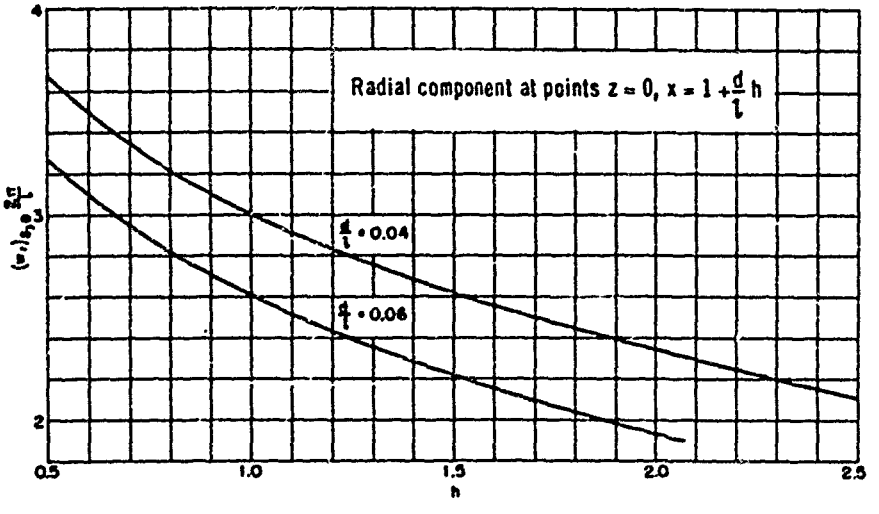

Figure 8a

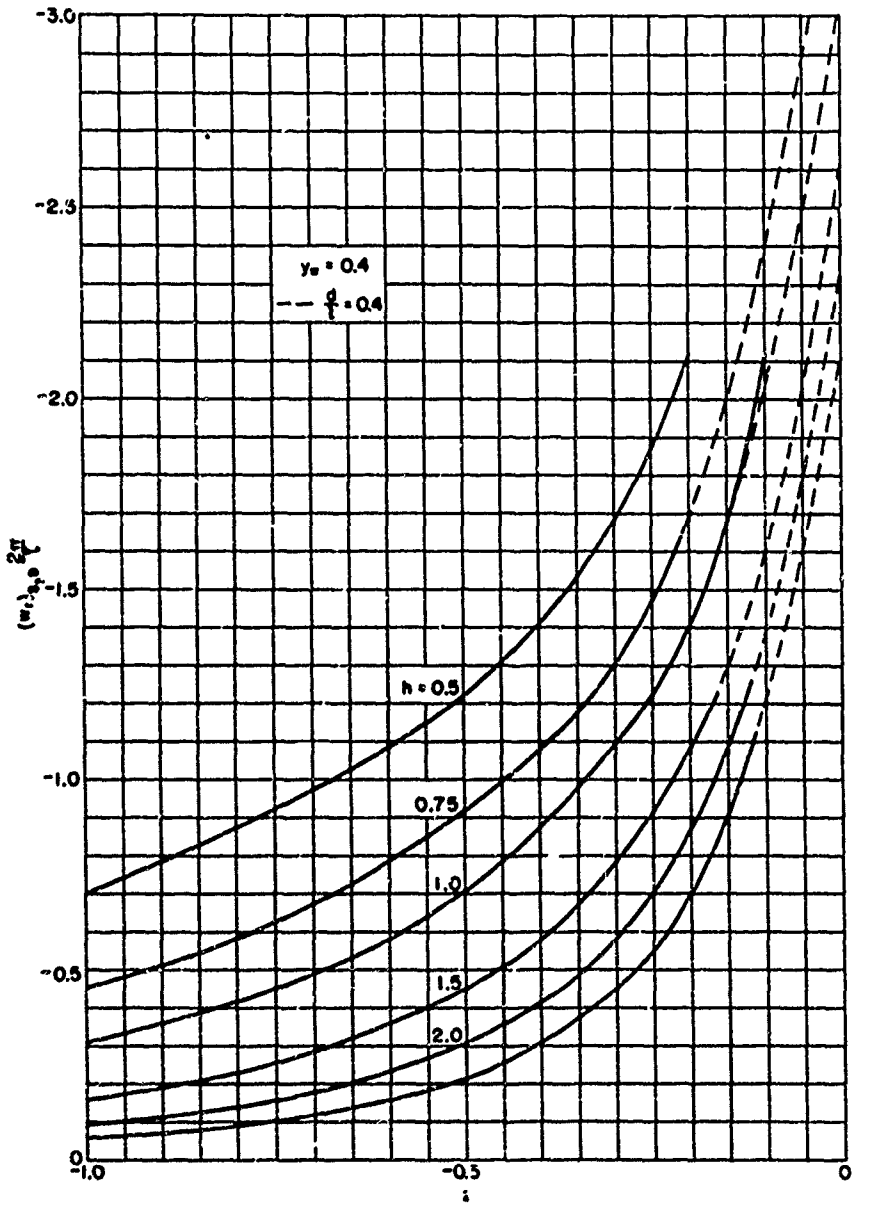

Figure 8b

For a sink disk of radius R with e_D assumed to be independent of the radius, the velocity potential ϕ at any point $r < R$ is represented in spherical coordinates r, ϑ, φ by the series

$$\phi_{(r,\vartheta)} = \frac{\bar{e}_D}{2} R\left(1 - \frac{r}{R} P_1 + \frac{1}{2} \frac{r^2}{R^2} P_2 - \frac{1}{8} \frac{r^4}{R^4} P_4 + \ldots\right)$$

$P_n = P_n(\cos\vartheta)$ is the Legendre polynomial of n^{th} degree. This potential satisfies Laplace's equation, the boundary conditions being the values of the potential at infinity and at the axis; the latter is known from a simple integration over the radius of the disk. By comparison, it is seen that these boundary conditions are identical with those of the gravitation potential of the disk; the details of this deduction are available in standard textbooks.

From the afore-written series for ϕ (which is independent of φ and, therefore, axisymmetrical), the axial velocity component at points arbitrarily near the disk $(\vartheta = \frac{\pi}{2} - \epsilon, \epsilon \to 0)$ becomes

$$(w_a)_{D,D} = \frac{1}{r}\left(\frac{\partial \phi}{\partial \vartheta}\right)_{\substack{\vartheta = \frac{\pi}{2} - \epsilon \\ \epsilon \to 0}} = \frac{\bar{e}_D}{2} \text{ for } r < R \qquad [5]$$

For points of reference for which $r > R$, the potential is represented by

$$\phi_{(r,\vartheta)} = \frac{\bar{e}_D}{2} R\left(\frac{1}{2} \frac{R}{r} - \frac{1}{8} \frac{R^3}{r^3} P_2 + \frac{1}{16} \frac{R^5}{r^5} P_4 - \ldots\right)$$

from which there is obtained for points arbitrarily near the plane of the disk

$$(w_a)_{D,D} = 0 \quad \text{for} \quad r > R \qquad [6]$$

If e_D is independent of the radius, the axial velocity component is constant over the disk and is zero outside of the disk for points within its plane.

Now compare the velocity field of a sink disk with that of a rotor. At the disk, the velocity jumps from $-(e_D)/2$ to $+(e_D)/2$; this follows from the afore-written velocity potentials. Otherwise, the velocity field of the sink disk is continuous. In particular, with respect to the axial component, it follows from Equation [3] that positive values of z (which are behind the disk) yield a negative quantity (w_a), $\bar{e}_D$ being a sink density. As compared to the absolute flow of a propeller, this holds for the velocity field behind the propeller outside of the slipstream but not within the slipstream. To approximate the slipstream behind the rotor with respect to the axial component, it is necessary to superimpose on the sink flow behind the disk a velocity field of magnitude $|\bar{e}_D|$ which is in the direction of positive z. Then the axial velocity component right behind the disk becomes $(|\bar{e}_D| - |\bar{e}_D|/2) = |\bar{e}_D|/2$ which equals the inflow into the disk. Infinitely far behind the disk, the effect from the sinks is zero and the velocity equals $|\bar{e}_D|$. Hence, the axial velocity of the combined flow behaves like the axial velocity component of a propeller, viz., it is continuous at the propeller and infinitely aft it increases to twice the value at the

propeller. Further, considering the axial component in the vicinity of a cylinder of radius R, the axial component of the absolute flow is continuous when traveling through the cylinder in front of the disk but discontinuous behind it. This complies with the properties of the axial velocity component of a propeller.

Behind the disk, the axial component of the absolute propeller flow jumps from $[|\bar{e}_D| + w_a(+z)]$ inside to $w_a(+z)$ outside of the race, and at the boundary it equals $[e_D/2 + w_a(+z)]$. Since $w_a(+z) = -w_a(-z)$ the axial component of the interference velocity at the shroud from the rotor for positive z expressed in terms of the sink flow becomes

$$w_a(+z)_{S,D} = \left|\frac{\bar{e}_D}{2}\right| - w_a(-z)_{S,D} \qquad [3c]$$

$w_a(-z)_{S,D}$ following from Figure 7.

In addition to the axial and radial velocity components, there is also a tangential velocity field from rotor and guide vanes which is caused by the hub vortices. When rotor and guide vanes are considered separately and the blades are replaced by lifting lines, the following conclusions are known from Stokes' Law with respect to the tangential velocity field of each of the components: The field is zero in front of the lifting lines and is

$$w_t = \frac{n\Gamma}{4r\pi} \qquad [7]$$

at a lifting line, where Γ is the circulation at one of the lifting lines and n is the number of blades on rotor or number of vanes. In the flow behind the respective component, the tangential velocity equals twice this value.

The velocity which is induced at the shaft sink from the sink disk follows from Equations [3a] or [3b] when introducing

$$x_{sh} = 0$$

$$z_{sh} = \frac{a_{sh}}{l/2} = \frac{l_{sh}}{l/2} - \frac{x_h}{2h}$$

and when adding the (negative) quantity so obtained to the uniform velocity field $|e_D|$. (Relative to the position of the shaft sink on the axis, see Section 2.3.)

When a sink density at the disk which is independent of the radius $\bar{e}_D$ is assumed, the nondimensional axial component at the shaft sink becomes

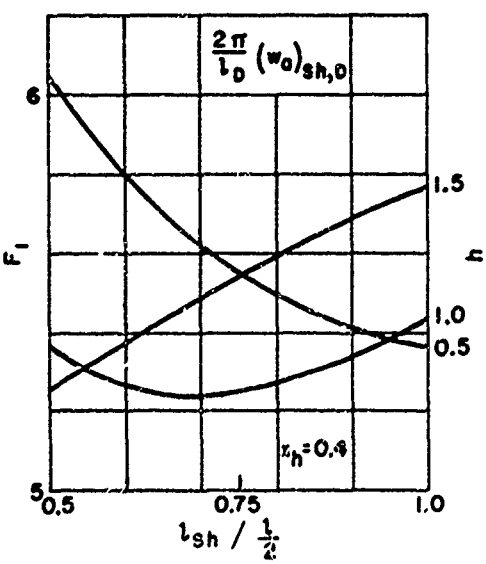

Figure 9

$$\frac{2\pi}{\bar{e}_D}(w_a)_{sh,D} = 2\pi - \int_{x_h}^{1} \frac{|w_a^*|}{x'}\,dx' = F_1 \qquad [3d]$$

This function F_1 is represented on Figure 9 for a range of the ratio $l_{sh}/(l/2)$, i.e., the ratio of the shaft length measured from $z = 0$ to the length of half the shroud, and for several values of h, x_h being chosen 0.4.

2.3 THE VELOCITY FIELD OF THE SHAFT SINK

The termination of the shaft requires a sink-source distribution on the axis. When this distribution is approximately replaced by a single sink, it follows from well-known relations, $x_h = R_{sh}/R$ being the nondimensional radius of the shaft, that

for the strength of the sink $$\frac{e_{sh}}{v_{sh}} = R^2 \pi x_h^2 \qquad [8]$$

for the position of the sink $$z_{sh} = \frac{z_{sh}}{l/2} = \frac{l_{sh}}{l/2} - \frac{1}{2}\frac{x_h}{h} \qquad [9]$$

These relations hold when the velocity v_{sh} is uniform. With the rotor and shroud working, the difficulty arises that the velocity field within which the shaft is situated is no longer uniform but depends on both the radial and axial coordinates. As an approximation, the sum of the velocity of approach and of the axial components which are induced at the place of the shaft sink from shroud and rotor will be introduced for v_{sh}

$$\frac{v_{sh}}{v_0} \doteq 1 - \frac{G_N}{(1 + z_{sh}^2 h^2)^{\frac{3}{2}}} + \frac{1}{2\pi}\left|\frac{\bar{e}_{II}}{v_0}\right| F_1 \qquad [10]$$

the function F_1 being represented on Figure 9.

This approximation does not satisfy the boundary condition that the normal component of the flow relative to the shaft is zero. The errors which arise should be checked afterwards by calculating the normal component of the combined flow on the given shaft contour.

With these relations for the shaft sink, one obtains for the velocity components which are induced at the shroud from the shaft sink

$$\left(\frac{w_a}{v_0}\right)_{s,sh} = -\frac{1}{4}\frac{v_{sh}}{v_0} x_h^2 \frac{h(z - z_{sh})}{\left[1 + h^2(z - z_{sh})^2\right]^{\frac{3}{2}}} \qquad [11a]$$

$$\left(\frac{w_r}{v_0}\right)_{s,sh} = -\frac{1}{4}\frac{v_{sh}}{v_0} x_h^2 \frac{1}{\left[1 + h^2(z - z_{sh})^2\right]^{\frac{3}{2}}} \qquad [11b]$$

The foregoing considerations and numerical evaluations give a sufficient knowledge of the velocity field of the shrouded propeller. This velocity field forms the basis for ascertaining the force components.

3. THE FORCES

As mentioned on page 3, the interaction forces result from the mutual interference velocities between the singularities. The interactions with the shaft sink will be omitted when determining these forces since these interactions are very small. Furthermore, these quantities cannot be determined very accurately because of the approximations for the strength of the sink. (The velocity field of the shaft sink will, however, be taken into account for the camber line of the shroud since in this case it is essential in order to satisfy the continuity equation.)

Disregarding the interactions with the shaft sink, the net thrust of the system will be obtained when the axial force on the shroud is subtracted from the thrust of rotor and guide vanes.

3.1 THE FORCES ACTING ON THE SHROUD

The axial force on the shroud vortices T_S arises from the radial velocity component which is induced at the shroud from other singularities present.

In this case, the singularities present are the sinks at the disk (which replace rotor and guide vanes) and the hub vortices. Since the direction of the velocity induced from the latter coincides with the direction of the vortex lines of the shroud, the effect on the force is zero. Then with the radial component from the sink disk $(w_r)_{S,D}$, the axial force becomes

$$T_{S,D} = 2\rho R^2 \pi h \int_{-1}^{+1} \gamma(z)(w_r)_{S,D}\, dz \qquad [12a]$$

With a positive $\gamma(z)$ [which represents the circulation per unit length over the shroud] and with an inward radial velocity component from the sink disk, the axial force on the shroud is directed backwards, i.e., this force represents a resistance.

Introducing for $\gamma(z)$ the elliptical distribution which is assumed in this paper, viz.,

$$\gamma(z) = \frac{4}{\pi} v_0 \frac{G_S}{h} \sqrt{1 - z^2}$$

one obtains for the nondimensional coefficient of the axial force on the shroud which is induced from the disk

$$(c_T)_{S,D} = \frac{T_{S,D}}{\frac{\rho}{2}\left(R^2 - r_h^2\right)\pi v_0^2} = \frac{16}{\pi\left(1 - x_h^2\right)} G_S \int_{-1}^{+1} \sqrt{1 - z^2}\left(\frac{w_r}{v_0}\right)_{S,D} dz \qquad [12b]$$

An alternative expression for this force can be deduced when considering the reaction of the sink disk to the interference velocity from the shroud vortices. From the remarks on page 3, this reaction force is equal to but opposite to that which is caused by the interference velocity from the sink disk at the shroud vortices and which is expressed by Equation [12a].

For this reaction force (denoted by $T_{D,S}$) in terms of quantities of the disk, the following is obtained

$$T_{D,S} = 2\rho\pi R^2 \int_{x_h}^{1} e_D(x)\,(w_a)_{D,S}\,x\,dx \qquad [13a]$$

$$(c_T)_{D,S} = \frac{4}{1-x_h^2}\int_{x_h}^{1} \frac{e_D(x)}{v_0}\left(\frac{w_a}{v_0}\right)_{D,S} x\,dx \qquad [13b]$$

$$|(c_T)_{S,D}| = |(c_T)_{D,S}| \qquad [14]$$

Both of the expressions [12b] and [13b] depend on the radial distribution of the sinks over the disk, Equation [13b] in a direct way and Equation [12b] by $(w_r)_{S,D}$ which, from Equation [4a], is related to $e_D(x)$. In order to evaluate Equations [12b] and [13b], the distribution $e_D(x)$ must be known. In the case that e_D is independent of x or can be replaced by an average $\bar{e}_D$, the force coefficients can be evaluated once and for all. In this case if follows that

$$(c_T)_{S,D}\,\frac{v_0}{G_S\,\bar{e}_D} = \frac{1}{1-x_h^2}\,\frac{8}{\pi^2}\int_{-1}^{+1}\sqrt{1-z^2}\left[(w_r)_{S,D}\,\frac{2\pi}{\bar{e}_D}\right]dz \qquad [12c]$$

and that

$$(c_T)_{D,S}\,\frac{v_0}{G_S\,\bar{e}_D} = \frac{4}{1-x_h^2}\int_{x_h}^{1}\left[\left(\frac{w_a}{v_0}\right)_{D,S}\frac{1}{G_S}\right]x\,dx \qquad [13c]$$

The factors in brackets are known from Figure 8 and Figure 2, respectively. The representation of these expressions on Figure 10 shows that Equation [14] holds within the accuracy of numerical integration which is limited by the properties of the integrands when z approaches zero and when x approaches 1. In the first case, the integrand becomes infinite since K becomes infinite as nat log (l/z) which necessitates, for numerical evaluation, the transformation $z = t^n$, $n > 1$.

In the following, the absolute value of the function which is defined by Equation [12c] or [13c] is denoted by F_2.

The radial force component on the shroud is determined from the axial velocity components which are induced at the shroud. Since this force is normal to the velocity of advance v_0, it does not affect the transformation of power input within the shrouded propeller and is,

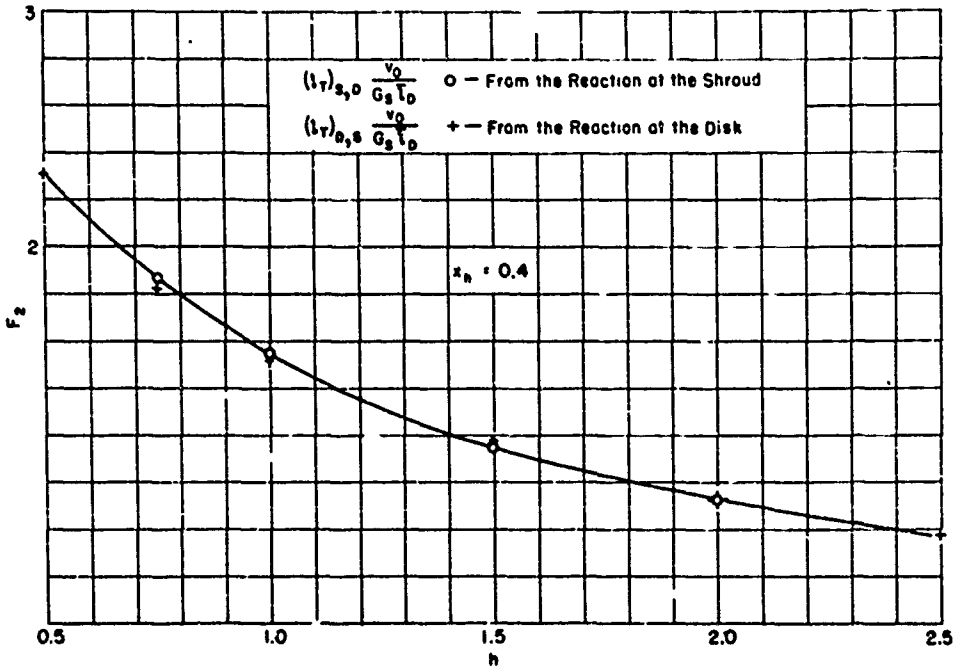

Figure 10 - Axial Reaction Force Between Shroud and Rotor

therefore, not evaluated. This force is significant, however, for considerations of the strength of the shroud.

3.2 THE FORCES ACTING ON THE ROTOR

As mentioned previously, the rotor is replaced by lifting lines in order to determine the forces at the rotor. Then the total force (including the reaction with the shroud) follows from Kutta's law, taking into account the resultant velocity field at a rotor lifting line.

The tangential velocity component is generated by the hub vortex of the rotor $n_R \Gamma_R$, and there are no parts within the tangential component either from the shroud (because of axial symmetry of the induced flow) or from the guide vanes (from the law of Stokes if the vanes are arranged behind the rotor). Then, from Equation [7], for the tangential velocity induced at the rotor

$$(w_t)_K = \frac{n_K \Gamma_K}{4\pi r} = \frac{n_K G_K}{x} \frac{v_0}{2\pi} \qquad [15]$$

With respect to the axial velocity component induced at a lifting line of the rotor, this component results from the shroud vortices and the sinks at the disk; the latter includes effects from the lifting lines of the guide vanes. Accordingly

$$(w_a)_R = (w_a)_{D,D} + (w_a)_{D,S} = \frac{\overline{e_D}}{2} + (w_a)_{D,S}$$

Within this expression, $(w_a)_{D,D}$ follows from Equation [5] and $(w_a)_{D,S}$ from Figure 2. It is seen from this diagram that $(w_a)_{D,S}$ is a negative quantity when the sense of circulation at the shroud is such that a pressure increase arises within the shroud, i.e., when γ is positive. Then $(w_a)_{D,D}$ is of the same direction as v_0 but $(w_a)_{D,S}$ is opposite.

With these expressions for the induced velocity components, the force elements at the rotor become

in axial direction $$(dT)_R = \rho(n_R\Gamma_R)\Big[\omega r - (w_t)_R\Big]dr \qquad [16]$$

in tangential direction $$(dQ)_R = \rho(n_R\Gamma_R)\Big[v_0 + \Big|\frac{\overline{e_D}}{2}\Big| - |(w_a)_{D,S}|\Big]dr \qquad [17]$$

Absolute values for the velocity components are introduced into the latter relation in order to avoid mistakes in the signs.

3.3 THE FORCES ACTING ON THE GUIDE VANES

Again, from Kutta's law, these forces follow from the velocity components. The axial velocity component being continuous, it equals the axial component at the rotor

$$(w_a)_V = (w_a)_R = \Big|\frac{\overline{e_D}}{2}\Big| - |(w_a)_{D,S}|$$

The tangential force component at the vanes which follows from the axial velocity component is without interest for the propulsion of the system.

The tangential velocity component at the vanes $(w_t)_V$ is determined from the condition that the guide vanes cancel the tangential velocity field of the rotor (which, however, is possible only with an infinite number of blades.) Behind the rotor, the tangential velocity equals $2(w_t)_R$, and behind the vanes, it equals $2(w_t)_V$. Therefore, to have the resultant tangential velocity zero in the slipstream, the following must hold

$$2(w_t)_V = -2(w_t)_R$$

That is, the total circulation at the guide vanes $n_V\Gamma_V$ is equal but opposite to that of the rotor $n_R\Gamma_R$, and the circulation of the respective hub vortices is equal but opposite. Then, the tangential component induced at the vanes from the hub vortex of the rotor equals $2(w_t)_R$ and that from the hub vortex of the vanes $-(w_t)_R$; hence, the resultant tangential velocity at the vanes equals

$$|(w_t)_V| = |(w_t)_R| = \frac{n_R \Gamma_R}{4r\pi} = \frac{n_R G_R}{x} \frac{v_0}{2\pi} \qquad [18]$$

From the last relation, one obtains for an element of the thrust at the vanes

$$(dT)_V = \rho(n_V \Gamma_V)(w_t)_V dr \qquad [19]$$

which is in the same direction as the thrust element on the rotor.

3.4 THE NET FORCE OF THE SYSTEM AND THE SINK DENSITY AT THE DISK

With the relations which have been established so far, expressions for both the net thrust of the system and for the power input can be established.

The net thrust T equals

$$T = T_R + T_V + T_S,$$

T_S, from Equation [12a], being a negative quantity for a positive γ.

Introducing Equations [13c], [15], [16], [18], and [19] gives for the coefficient of the net thrust

$$c_T = \frac{T}{\frac{\rho}{2}(R^2 - r_h^2)\pi v_0^2} = \frac{2}{\pi} \frac{n_R G_R}{\lambda} - G_S \left| \frac{\overline{e_D}}{v_0} \right| F_2 \qquad [20]$$

the negative sign being necessary when introducing the absolute values $|e_D|$ and F_2.

An expression for the power input P is deduced from Equation [17] in connection with Equation [13c]

$$c_P = \frac{P}{\frac{\rho}{2}(R^2 - r_h^2)\pi v_0^3} = \frac{2}{\pi} \frac{n_R G_R}{\lambda} \left[1 + \frac{1}{2} \left| \frac{\overline{e_D}}{v_0} \right| - \frac{F_2}{2} G_S \right] \qquad [21]$$

In order to establish an expression for the sink density at the disk, we refer to the law of momentum which states that the time rate of change of momentum equals the net thrust of the system. Since the scheme which has been constructed for representing the rotor flow leads to the result that the absolute axial velocity equals $|\overline{e_D}|$ in the final wake, the change of momentum of the mass per unit time dm equals $(\overline{e_D} dm)$. With

$$dm = \rho 2r\pi dr \left[v_0 + (w_a)_R \right] = \rho 2r\pi dr \left[v_0 + \left| \frac{\overline{e_D}}{2} \right| - |(w_a)_{R,S}| \right]$$

the law of momentum yields the relation

$$T = 2\rho\pi \int_{r_h}^{R} |\overline{e_D}| \left[v_0 + \left| \frac{\overline{e_D}}{2} \right| - |(w_a)_{R,S}| \right] r dr$$

In general, e_D will be a function of the radial coordinate x. To maintain the simple scheme of a circular sheet of vortices which is concentrated within the boundary of the rear jet, it is necessary to introduce an average of e_D over the radius. The reason for this is that a concentrated circular vortex sheet is equivalent to a uniform sink density over the disk, as mentioned previously. Otherwise, to account for a radially varying sink density, additional free vortex sheets, i.e., a radially varying circulation at the bound vortices, must be introduced which complicates the calculations considerably.

The average $\overline{e}_D$ is determined such that the net thrust from Equation [20], which is the arithmetic sum of the axial forces on the substituted bound vortices, equals the net thrust from the law of momentum. This leads to the relation

$$\left|\frac{\overline{e_D}}{v_0}\right| = \sqrt{1 + \frac{2}{\pi}\,\frac{n_R G_R}{\lambda}} - 1 \qquad [22]$$

3.5 RELATIONS FOR THE CIRCULATION AT ROTOR, SHROUD, AND GUIDE VANES

When the required net thrust of the system is a given quantity, Equation [20] represents a relation between c_T and the unknowns G_R and G_S. The same holds for Equation [21] when the power input is a given quantity.

A condition for G_S is found from the required pressure increase in the plane of the rotor $\Delta p = p_R - p_0$. This pressure increase is related to the flow within which the rotor is located and whose axial component in the plane of the rotor amounts to $[v_0 - |(w_a)_{D,S}|]$. Then, it follows from Bernoulli's equation that

$$\frac{\Delta p}{\frac{\rho}{2} v_0^2} = 1 - \left[1 - G_S \left|\left(\frac{w_a}{v_0}\,\frac{1}{G_S}\right)_{D,S}\right|\right]^2 \qquad [23]$$

from which the circulation at the shroud is represented by

$$G_S = \frac{1 - \sqrt{1 - \frac{\Delta p}{\rho/2\, v_0^2}}}{\left|\left(\frac{w_a}{v_0}\,\frac{1}{G_S}\right)_{D,S}\right|} \qquad [23b]$$

Since the induced velocity $[(w_a/v_0)\,(1/G_S)]_{D,S}$ depends on the radius, the required pressure increase should be related to a certain radius.

The loading coefficient c_T or c_P and, further, $\Delta p/(\rho/2)v_0^2$, n_R, and λ are considered given quantities. Then one obtains the circulation at the shroud G_S from Equation [23b]

and, with this value for G_S, the circulation G_R from Equation [20] or [21] together with [22]. The equation for $(n_R G_R)$ so obtained reads in terms of the thrust coefficient

$$\left(\frac{n_R G_R}{\lambda}\right)^2 - \left(\frac{n_R G_R}{\lambda}\right) \pi \left[(c_T - G_S F_2) + \frac{G_S^2 F_2^2}{2}\right] + c_T \frac{\pi^2}{4} (c_T - 2 G_S F_2) = 0 \qquad [24]$$

or in terms of the power coefficient

$$\left(\frac{n_R G_R}{\lambda}\right)^3 + \left(\frac{n_R G_R}{\lambda}\right)^2 \pi G_S F_2 \left(1 - \frac{G_S F_2}{2}\right) + \left(\frac{n_R G_R}{\lambda}\right) \pi^2 c_P (1 - G_S F_2) - \frac{\pi^3}{2} c_P^2 = 0 \qquad [25]$$

The circulation at the rotor being known, the circulation at the guide vanes equals the total circulation at the rotor from reasons mentioned previously. Therefore

$$n_V G_V = n_R G_R \qquad [26]$$

4. DESIGN DATA FOR ROTOR, GUIDE VANES, AND SHROUD

4.1 ROTOR

Expressing the lift on an element of a rotor blade by the law of Kutta-Joukowsky and, on the other hand, by the lift coefficient, and equating the expressions, the following obtains

$$(c_L l)_R = 2 \frac{\Gamma_R}{V_R}$$

where the resultant relative velocity at the station r of the blade is expressed by

$$V_R^2 = \left[v_0 + \left|\frac{\overline{e_D}}{2}\right| - |(w_a)_{D,S}|\right]^2 + [\omega_r - (w_t)_R]^2$$

Nondimensionally, these expressions read

$$\frac{(c_L l)_R}{D} = 2 \left(\frac{v_0}{V_R}\right) G_R$$

$$\left(\frac{V_R}{v_0}\right)^2 = \left[1 + \frac{1}{2}\left|\frac{\overline{e_D}}{v_0}\right| - G_S \left|\left(\frac{w_a}{v_0} \frac{1}{G_S}\right)_{D,S}\right|\right]^2 + \left[\frac{x}{\lambda} - \frac{n_R G_R}{2x\pi}\right]^2 \qquad [27]$$

The density e_D/v_0 is known from Equation [22], the axial induction from the shroud $|[(w_a/v_0)\,(1/G_S)]_{D,S}|$ from Figure 2.

In connection with the last two relations, the direction of the relative velocity by which the position of the section is fixed follows from the relation (see Figure 11) :

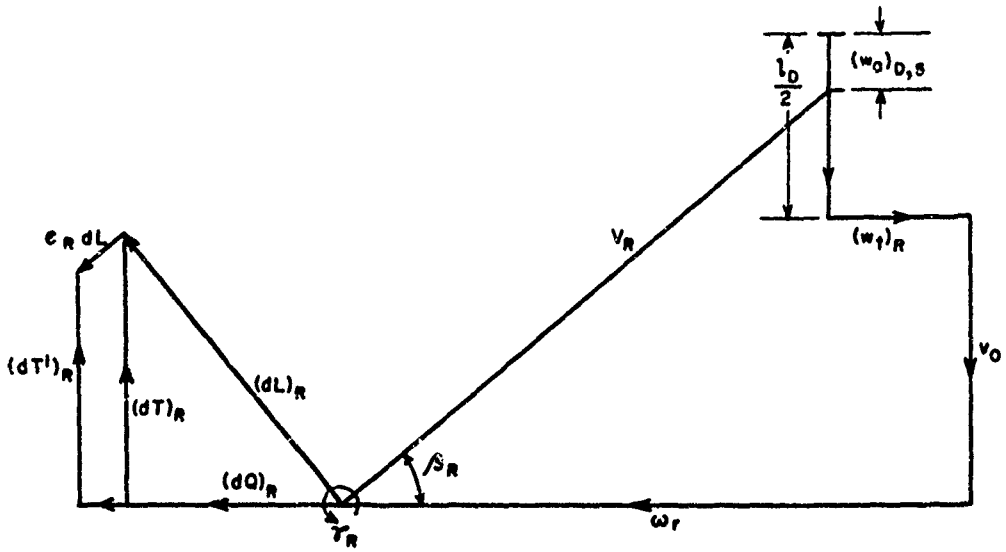

Figure 11 - Velocity and Force Diagram at a Section of the Rotor

$$\tan \beta_R = \frac{1 + \frac{1}{2}\left|\frac{\bar{e}_D}{v_0}\right| - G_S\left|\left(\frac{w_a}{v_0}\frac{1}{G_S}\right)_{D,S}\right|}{\frac{r}{\lambda} - \frac{n_R G_R}{2\pi}} \qquad [28]$$

Further, in the design of the rotor, its local cavitation number must be known. This is given by the expression

$$\begin{aligned}
\sigma_R &= \frac{\left(p_R - \rho\int_r^R w_t^2\,\frac{dr}{r}\right) - p^*}{\frac{\rho}{2}V_R^2} \\
&= \left(\frac{v_0}{V_R}\right)^2\left\{\sigma_0 + \frac{\Delta p}{\frac{\rho}{2}v_0^2} - 2\int_x^1\left(\frac{w_t}{v_0}\right)^2\frac{dx}{x}\right\} \\
&= \left(\frac{v_0}{V_R}\right)^2\left[\sigma_0 + \frac{\Delta p}{\frac{\rho}{2}v_0^2} - \left(\frac{n_R G_R}{2\pi}\right)^2\left(\frac{1}{x^2} - 1\right)\right]
\end{aligned} \qquad [29]$$

$$\sigma_0 = \frac{(\quad - p^*)}{\left(\frac{}{2}v_0^2\right)}$$

where σ_0 is the cavitation number of the undisturbed flow.

Cavitation will not take place on a section of the rotor if

$$\sigma_R \geqq \left| \frac{p - p_0}{\frac{\rho}{2} v_0^2} \right|_{min}$$

where the term on the right-hand side denotes the absolute value of the nondimensional minimum of the pressure on the section.

By means of these formulas, the design of the rotor follows usual procedure, viz., to determine c_L and l so that the calculated product $(c_L\ l)$ is satisfied and that, at the same time, the onset of cavitation is avoided. This requires knowledge of both lift versus angle of attack curves and pressure distribution curves of sections in cascade. On the other hand, the knowledge of two-dimensional cascade effects on the sections is sufficient for this problem since the flow at the rotor for a constant circulation is essentially two-dimensional (in contrast to the unshrouded propeller where the flow is essentially three-dimensional).

4.2 GUIDE VANES

Analogously as for the rotor, there is obtained

$$(c_L\, l)_V = 2\, \frac{\Gamma_V}{V_V} = 2\, \frac{n_R}{n_V}\, \frac{\Gamma_R}{V_V}$$

since the condition of Equation [26] must be true in order to cancel the tangential velocity field of the rotor by means of the vanes. In this flow condition, the resultant relative velocity at the vanes V_V is expressed by

$$V_V^2 = \left[v_0 + \left| \frac{\bar{e}_D}{2} \right| - (w_a)_{D,S} \right]^2 + (w_t)_R^2$$

Nondimensionally, the last two relations become

$$\frac{(c_L\, l)_V}{D} = 2\, \frac{n_R}{n_V} \left(\frac{v_0}{V_V} \right) G_R$$

$$\left(\frac{V_V}{v_0} \right)^2 = \left[1 + \frac{1}{2} \left| \frac{\bar{e}_D}{v_0} \right| - G_S \left| \left(\frac{w_a}{v_0}\, \frac{1}{G_S} \right)_{D,S} \right| \right]^2 + \left(\frac{n_R G_R}{2\pi x} \right)^2 \qquad [30]$$

The angle β_V of the resultant relative velocity at the vanes with the plane of the rotor is determined from the following equation (see Figure 12)

$$\tan \beta_V = 2\pi x\, \frac{1 + \frac{1}{2} \left| \frac{\bar{e}_D}{v_0} \right| - G_S \left| \left(\frac{w_a}{v_0}\, \frac{1}{G_S} \right)_{D,S} \right|}{n_R\, G_R} \qquad [31]$$

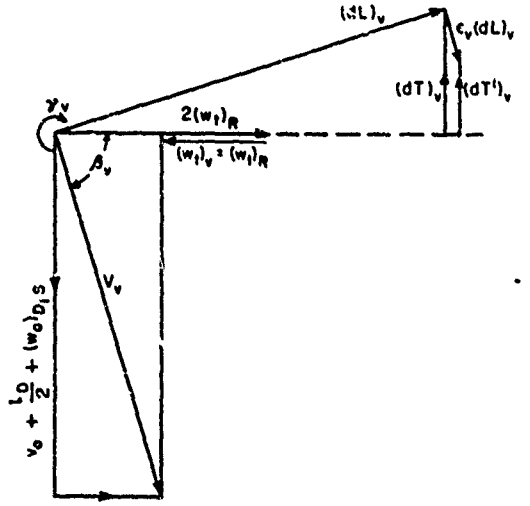

Figure 12 - Velocity and Force Diagram at a Section of the Guide Vanes

For the local cavitation number at the vanes, the following obtains

$$\sigma_V = \frac{\left(p_v - \rho\int_r^R w_t^2 \frac{dr}{r}\right) - p^*}{\frac{\rho}{2} V_v^2} \doteq \sigma_R \left(\frac{V_R}{v_0}\right)^2 \left(\frac{v_0}{V_v}\right)^2 \qquad [32]$$

if the approximation $p_V = p_R$ is applied.

4.3 SHROUD

In accordance with thin airfoil theory, the shroud section is considered to consist of an infinitely thin, camber line section (which produces circulation) and of a superimposed thickness form, the combined effect of which on the velocity distribution is obtained when adding the individual effects. In the following treatment, the shape of the camber line and its position relative to the undisturbed flow, i.e., its geometric angle of attack, are first determined so that an elliptic distribution of circulation is realized on the shroud, and then a thickness function in axisymmetrical flow is considered.

The shape of the camber line follows from the boundary condition that the velocity vector at the camber line is tangent to this line, i.e., that this line represents a streamline of the flow. The flow at the camber line is a result of the velocity of approach, the self-induction of the shroud, and the inductions from both the sink disk and the shaft sink. Consequently, the axial component of the resultant flow amounts to

$$v_0 + (w_a)_{S,S} + (w_a)_{S,D} + (w_a)_{S,sh}$$

and the radial component to

$$(w_r)_{S,S} + (w_r)_{S,D} + (w_r)_{S,sh}$$

The camber line , with coordinates a and $(r - R)$, is a streamline if

$$\frac{dr}{da} = \frac{(w_r)_{S,S} + (w_r)_{S,D} + (w_r)_{S,sh}}{v_0 + (w_a)_{S,S} + (w_a)_{S,D} + (w_a)_{S,sh}}$$

In this relation, the induction from the shaft sink has been allowed for in order to have the continuity equation satisfied.

Introducing the nondimensional coordinates

$$y = \frac{r - R}{l/2} \quad \text{and} \quad z = \frac{a}{l/2}$$

gives a first-order differential equation for the shape of the camber line $y = y(z)$

$$dy = \frac{G_S\left(\frac{w_r}{v_0}\frac{1}{G_S}\right)_{S,S} + \frac{1}{2\pi}\frac{\bar{e}_D}{v_0}\left[(w_r)_{S,D}\frac{2\pi}{\bar{e}_D}\right] + \left(\frac{w_r}{v_0}\right)_{S,sh}}{1 + G_S\left(\frac{w_a}{v_0}\frac{1}{G_S}\right)_{S,S} + \frac{1}{2\pi}\frac{\bar{e}_D}{v_0}\left[(w_a)_{S,D}\frac{2\pi}{\bar{e}_D}\right] + \left(\frac{w_a}{v_0}\right)_{S,sh}} dz \qquad [33]$$

in which relation the terms are determined by the equations or diagrams as listed in the table on page 30. The table also indicates the sign of the respective velocity components for a positive circulation at the shroud and for a sink density at the disk.

From Equations [3] and [4], the integrands of both $(w_a)_{S,D}$ and $(w_r)_{S,D}$ become infinite for $x = 1$ when z becomes zero, i.e., when the point of reference coincides with the edge of the sink disk. These infinities arise from the assumption that the vortices of the shroud are situated on the disk cylinder instead of being arranged on the camber line. This means that in the neighborhood of $z = 0$, the finite distance $d/2$ between camber line and disk cylinder should be taken into account although it can be neglected outside of a certain interval around $z = 0$. For this reason, the induction at the shroud from the disk as represented on Figures 7 and 8 can be considered accurate in an interval of z between ± 1 and z about ± 0.2, the last figure being obtained from comparative calculations of the velocity components at lines $r = R + d/2$ and $r = R$.

Between $z = +0.2$ and $z = -0.2$, the induced velocity components as represented on Figures 7 and 8 are exaggerated. With respect to the integrand of Equation [33] which must be known within the entire interval from $z = -1$ to $z = +1$, a close approximation is obtained when reading off $(w_r)_{S,D}$ between $z = -0.2$ and $z = 0$ on the dotted curves of Figure 8. For these dotted curves, the radial distance of the points of reference equals $(R + d/2)$, i.e., $x = 1 + (d/l)h$; these points are very close to the camber line around $z = 0$.

Velocity Component		Sign for $-s$	Sign for $+s$
$\left(\frac{w_r}{v_0}\frac{1}{G_S}\right)_{S,S}$	Figure 4	+	−
$(w_r)_{S,D}\frac{2\pi}{\overline{\overline{e}}_D}$	Figure 8 Figure 8a	−	−
$\left(\frac{w_r}{v_0}\right)_{S,sh}$	Equations [10] and [11b]	−	−
$\left(\frac{w_a}{v_0}\frac{1}{G_S}\right)_{S,S}$	Figure 8	−	−
$(w_a)_{S,D}\frac{2\pi}{\overline{\overline{e}}_D}$	Figure 7, Equation [3c]	+ (Figure 7)	+ (Equation [3c])
$\left(\frac{w_a}{v_0}\right)_{S,sh}$	Equations [10] and [11a]	+ when $s<s_{sh}$	− when $s>s_{sh}$

To allow for the influence of the thickness of the shroud, the calculations have been made for $d/l = 0.04$ and $d/l = 0.06$ (Figure 8a); these curves are so related that equal coordinates are obtained for equal quantities $(d/l)\bar{h}$.

For $(w_a)_{S,D}$, this component equals zero at the point with coordinates $s = 0$ and $x = 1 + (d/l)\bar{h}$. Since this component occurs within a sum, together with the relatively greater number 1, it is sufficiently accurate to interpolate this sum between $s = -0.2$ and $s = +0.2$ from the known values at $s = -0.2$ and $s = +0.2$.

In this way, a closer approximation to the velocity field at the camber line of the shroud is obtained than by replacing the sink disk by a point disk at the axis, the strength of which is such that the sink disk and the point sink are acted on by an equal interaction force from the shroud. This approximation has been proposed by Horn for the purpose of determining the circulation at a Kort nozzle.[5] The two velocity fields, however, differ greatly in the vicinity of the shroud and become sufficiently coincident only at a great distance from the disk.

The integration of Equation [33] requires the determination of an integration constant from the given ordinate of the camber line at an arbitrary station s. Corresponding to the geometric configuration of the propulsion system, this constant is chosen so that $y = d/2$ for $s = 0$. With this, a first approximation for the shape and for the geometric angle of attack

of the camber line is obtained when integrating Equation [33] by numerical methods. A second approximation follows when arranging the vortices of the shroud on the first approximation for the camber line and when calculating the velocity components which occur in Equation [33] on the camber line instead of on the rotor cylinder. The previously mentioned tables by Kuechemann are very useful for this purpose.[4] The velocity components which are induced at the first approximation of the shroud, both from the sink disk and from the shroud itself, can be ascertained within a reasonable amount of time by applying these tables.

The maximum velocity (or the minimum pressure) on the shroud must be known in order to determine the cavitation number of the shroud. Following the procedure with thin airfoils, a close approximation to the velocity distribution on the shroud is obtained when adding the velocities on the infinitely thin camber line section and those on the thickness shape. An additional velocity distribution associated with angle of attack need not be considered since the shroud is supposed to work in the shock-free flow condition.

By definition, the thickness form produces no lift at zero angle of attack. Therefore, in two-dimensional flow, it is symmetrical about the direction of the undisturbed velocity. For the same reason, the velocity field of the thickness shape can be represented by a suitable sink-source distribution on the axis of symmetry of the section. This method is also applicable to the thickness function of a ring-shaped hydrofoil (in contrast to the method of conformal mapping which is restricted to two-dimensional flow). Kuechemann has investigated the effect of axial symmetry in this way, assuming ring-shaped sink-source distributions by which, in the case of two-dimensional flow, symmetrical Joukowsky profiles are generated.[6] In the axisymmetrical case, the generated annular sections are no longer symmetrical about the direction of the undisturbed flow but have a curved middle line; the camber increases when the ratio of thickness to chord-length d/l increases. The influence on the pressure distribution is shown by Kuechemann on annular half-bodies (which are generated by a ring source within the undisturbed flow) from which it follows that the pressure distribution on the body is no longer symmetrical in a meridian plane but the peak of suction is greater inside than outside, the asymmetry increasing with thickness.

It follows from these investigations that when taking a thickness form whose pressure distribution is known in two-dimensional flow (*e.g.*, one of the NACA basic thickness forms), we cannot rely immediately on the two-dimensional pressure distribution in axisymmetrical flow. In order to ascertain the difference of the pressure distribution for the same section in these two cases, it has been attempted, by means of Equations [3] and [4], to determine a distribution of ring-shaped sinks and sources on the axis so that the thickness form becomes a streamline. In the analogous two-dimensional problem, the sink-source distribution follows from an integral equation. In the case of axial symmetry, it has not been possible yet to establish the corresponding integral equation because of complications which arise from the expressions [3] and [4].

Although present knowledge does not permit comparison of sections of equal shape

in the two flow conditions, an idea of the order of magnitude of the influence of axial symmetry is obtained when comparing sections of equal sink-source distribution. Since the influence on both the shape and the pressure distribution increases with increasing thickness, it is of interest to know whether or not a thickness can be determined below which these influences are so small that they can be neglected. Taking the afore-mentioned sink-source distributions which, in the two-dimensional case, lead to symmetrical Joukowsky profiles, the results are as follows: Below d/l about 0.08, the differences in pressure distribution as compared with the two-dimensional section of equal thickness chord-length ratio are negligibly small in the range of h investigated (0.7 to 2.1). Further, within this range of d/l and h, the deformation of the contour is allowed for with sufficient accuracy by a curvature of the middle line of the section without appreciable change of the ordinates, the latter being referred to the middle line. The curvature is small and in the interval investigated, it depends linearly on d/l, increasing slightly when h increases (Figure 13).

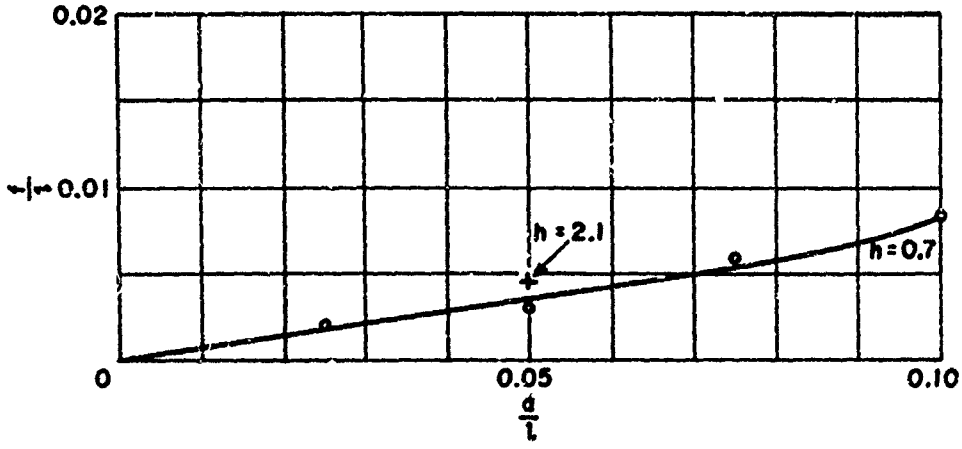

Figure 13 - Camber of Thickness-Forms in Axisymmetrical Flow

It is concluded from these calculations that the two-dimensional pressure distribution of a thin thickness form (d/l being not greater than about 0.08) can be applied for axisymmetrical flow if the thickness form is given a slight curvature corresponding to Figure 13.

An expression for the minimum pressure on the shroud can be deduced on this basis. Within the assumptions of linearized thin airfoil theory, the velocity at any point of the shroud is the sum of the velocities from the circulation distribution on the camber line and from the thickness form: $V = V_S + V_T$.

The latter is assumed to be known, e.g., from one of the NACA thickness forms; the former is the velocity just outside or inside of the camber line, i.e., just outside or inside of the vortex sheet. Let w_0 be the velocity at a point of the outside surface with axial coordinate z, and w_i the velocity at a point of the inside surface with the same axial coordinate. Then

$$w_0 - w_i = \gamma$$

where γ is the circulation per unit length at z. Further, just on the outside of the vortex cylinder, the relation

$$w_a = w_{\text{Sheet}} + w'$$

holds, and just on the inside at a point of equal z

$$w_i = w_{\text{Sheet}} - w'$$

where w' is the increment of velocity as compared to the velocity within the vortex sheet at equal z. From those relations, it follows for the unknown velocity w'

$$w' = \frac{1}{2}(w_a - w_i) = \frac{\gamma}{2}$$

Then, at a point on the outside of the camber line where, with a positive γ, the smallest pressures are found, the following obtains

$$\left(\frac{V_S}{v_0}\right)^2 = \left[1 + G_S\left(\frac{w_a}{v_0}\frac{1}{G_S}\right)_{S,S} + \frac{1}{2\pi}\left|\frac{\bar{e}_D}{v_0}\right|\left(w_n \frac{2\pi}{\bar{e}_D}\right)_{S,D} + \frac{2}{\pi}\frac{G_S}{h}\sqrt{1-z^2}\cos\alpha\right]^2$$

$$+ \left[G_S\left(\frac{w_r}{v_0}\frac{1}{G_S}\right)_{S,S} + \frac{1}{2\pi}\left|\frac{\bar{e}_D}{v_0}\right|\left(w_r \frac{2\pi}{\bar{e}_D}\right)_{S,D} - \frac{2}{\pi}\frac{G_S}{h}\sqrt{1-z^2}\sin\alpha\right]^2 \qquad [34]$$

The angle α is the declination of the camber line with respect to the z-axis which is small.

Relative to the values of $(w_a)_{S,D}$ and of $(w_r)_{S,D}$ in the interval of z between $z = -0.2$ and $z = +0.2$, see the explanation given in connection with Equation [33].

The velocity distribution V_T/v_0 is known for the thickness form. Then the maximum of the velocity at a shroud of finite but small thickness becomes

$$\left(\frac{V}{v_0}\right)_{\max} = \left(\frac{V_S}{v_0} + \frac{V_T}{v_0}\right)_{\max}$$

In order to avoid the onset of cavitation on the shroud, the following relation must be satisfied for the cavitation number of the oncoming flow

$$\sigma_0 = \frac{p_0 - p^*}{\rho/2 v_0^2} \geq \left(\frac{V}{v_0}\right)^2_{\max} - 1 \qquad [34a]$$

5. INFLUENCE OF VISCOUS FLOW ON THE FORCES AND ON THE EFFICIENCY

From Figure 11, it follows for the rotor when the respective forces in viscous flow are denoted by a prime

$$(dT)_R' = (dT)_R - (dD)_R \sin\beta_R = (dT)_R - \epsilon_R (dL)_R \sin\beta_R$$

$$= (dT)_R - \epsilon_R \frac{(dT)_R}{\cos\beta_R} \sin\beta_R = (dT)_R (1 - \epsilon_R \tan\beta_R)$$

$$(dQ)_R' = (dQ)_R + (dD)_R \cos\beta_R = (dQ)_R \left(1 + \frac{\epsilon_R}{\tan\beta_R}\right)$$

Within these expressions, ϵ_R is the drag-lift ratio at the section of the rotor under consideration.

Analogously, one obtains from Figure 12 for a section of the guide vanes

$$(dT)_V' = (dT)_V - (dD)_V \sin\beta_V = (dT)_V (1 - \epsilon_V \tan\beta_V)$$

At the shroud, the viscous drag of the shroud and the (nonviscous) interaction forces are in the same direction when γ is a positive quantity. In this case, the total drag of the shroud becomes

$$T_S' = T_S + D_S$$

or, nondimensionally,

$$(c_T)_S' = \frac{T_S'}{\frac{\rho}{2}(R^2 - r_h^2)\pi v_0^2} = (c_T)_S + (c_D)_S \frac{4h}{1 - x_h^2}$$

if $(c_D)_S$, as usual, is referred to the surface of the shroud $2R\pi l$.

The forces on rotor and vanes can be integrated when it is assumed that the drag-lift coefficients are independent of the radius. Introducing relations [16], [17], and [19] for the nonviscous parts of the forces, and relations [28] and [31] for the angles, one obtains

$$(c_T)_R' = (c_T)_R - \epsilon_R \frac{4}{\pi} \frac{n_R G_R}{1 - x_h^2} \left[\left(1 + \frac{1}{2}\left|\frac{\overline{e_D}}{v_0}\right|\right)(1 - x_h) - G_S \int_{x_h}^{1} \left| \left(\frac{w_a}{v_0} \frac{1}{G_S}\right)_{D,S} \right| dx \right] \quad [35]$$

$$(c_P)' = (c_P) + \epsilon_R \frac{2}{\pi} \frac{1}{\lambda} \frac{n_R G_R}{1 - x_h^2} \left[\frac{2}{3\lambda}(1 - x_h^3) - \frac{n_R G_R}{\pi}(1 - x_h) \right] \quad [36]$$

$$(c_T)_V' = (c_T)_V - \epsilon_V \frac{4}{\pi} \frac{n_R G_R}{1 - x_h^2} \left\{ \left(1 + \frac{1}{2} \left| \frac{\overline{e_D}}{v_0} \right| \right) (1 - x_h) - G_S \int_{x_h}^{1} \left| \left(\frac{w_a}{v_0} \frac{1}{G_S} \right)_{D,S} \right| dx \right\} \quad [37]$$

It follows for the coefficient of the net thrust c_T' that

$$c_T' = (c_T)_R' + (c_T)_V' - (c_T)_S' = c_T - (\epsilon_R + \epsilon_1) \frac{4}{\pi} \frac{n_R G_R}{1 - x_h^2}$$
$$\left[\left(1 + \frac{1}{2} \left| \frac{\overline{e_D}}{v_0} \right| \right) (1 - x_h) - G_S \int_{x_h}^{1} \left| \left(\frac{w_a}{v_0} \frac{1}{G_S} \right)_{D,S} \right| dx \right] - (c_D)_S \frac{4h}{1 - x_h^2} \quad [38]$$

With these expressions for c_T' and c_P', the efficiency of the system becomes

$$\eta = \frac{c_T'}{c_P'} = \eta_i \eta_e$$

where the ideal efficiency η_i is obtained when the expressions [20] and [21] for c_T and c_P are introduced

$$\eta_i = \frac{c_T}{c_P} = \frac{1 - \frac{\pi}{2} \lambda \frac{G_S}{n_R G_R} F_2 \left| \frac{\overline{e_D}}{v_0} \right|}{1 + \frac{1}{2} \left| \frac{\overline{e_D}}{v_0} \right| - \frac{G_S}{2} F_2} \quad [39]$$

For $G_S = 0$ (unshrouded propeller), this expression for η_i equals that from simple momentum theory. This is necessary because of the assumptions that the guide vanes cancel the tangential velocity field entirely and that the circulation is independent of the radius; these are just the assumptions of simple momentum theory.

For the reduction of the ideal efficiency due to drag, one obtains

$$\eta_e = \frac{1 - 2 \frac{(\epsilon_R + \epsilon_V) n_R G_R \left[\left(1 + \frac{1}{2} \left| \frac{\overline{e_D}}{v_0} \right| \right) (1 - x_h) - G_S \int_{x_h}^{1} \left| \left(\frac{w_a}{v_0} \frac{1}{G_S} \right)_{D,S} \right| dx \right] + (c_D)_S \pi h}{(1 - x_h^2) \left(\frac{n_R G_R}{\lambda} - \frac{\pi}{2} G_S F_2 \left| \frac{\overline{e_D}}{v_0} \right| \right)}}{1 + \frac{\epsilon_R}{1 - x_h^2} \frac{\frac{2}{3\lambda} (1 - x_h^3) - \frac{n_R G_R}{\pi} (1 - x_h)}{1 + \frac{1}{2} \left| \frac{\overline{e_D}}{v_0} \right| - \frac{G_S}{2} F_2}} \quad [40]$$

Assuming the conditions of an unshrouded propeller without guide vanes, viz., $G_S = 0$, $(c_D)_S = 0$, $\epsilon_V = 0$ and, further, putting $x_h = 0$, it follows from the last relation that

$$\eta_e = \frac{1 - 2 \epsilon_R \lambda \left(1 + \frac{1}{2} \left| \frac{\overline{e_D}}{v_0} \right| \right)}{1 + \frac{2}{3} \frac{\epsilon_R}{\lambda \left(1 + \frac{1}{2} \left| \frac{\overline{e_D}}{v_0} \right| \right)} - \epsilon_R \frac{n_R G_R}{1 + \frac{1}{2} \left| \frac{\overline{e_D}}{v_0} \right|}},$$

The third term in the denominator is small compared to 1 and can be neglected. Further,

$$\lambda\left(1+\frac{1}{2}\left|\frac{\overline{c_\mu}}{v_0}\right|\right) = \lambda\left(1+\frac{w_a}{v_0}\right) \doteq \lambda_i$$

Then, from the above expression, the well-known approximate formula for η_ϵ of an unshrouded propeller which has been deduced by von Kármán and Bienen is obtained:

$$\eta_\epsilon \doteq \frac{1-2\epsilon_R\lambda_i}{1+\frac{2}{3}\frac{\epsilon_R}{\lambda_i}}$$

It is difficult to draw general conclusions from the relations for the efficiencies. For a special case, viz., that for the low-speed pumpjet for DD 710, Model 3246, the following design data are given

$$c_\mu' = 1.08, \quad \lambda = 0.45, \quad \frac{\Delta_p}{\frac{\rho}{2}v_0^2} = 0.3, \quad h = 1.2$$

By means of successive approximations as described in section 7 of this report, the following obtains

$$\epsilon_R = \left(\frac{c_D}{c_L}\right)_R = 0.028, \quad \epsilon_V = \left(\frac{c_D}{c_L}\right)_V = 0.022$$

For determining these drag-lift coefficients, the drag coefficients $(c_D)_R = 0.010$ and $(c_D)_V = 0.024$ have been introduced, corresponding to the respective Reynolds numbers and angles of attack. The latter figure is greater than the former since the sections of the vanes work at a great lift coefficient with which a great pressure resistance is connected. In addition, the Reynolds number of the sections of the vanes is smaller than that of the rotor; because of this, the frictional coefficient becomes greater.

Assuming $(c_D)_S = 0.013$ (which figure, however, is uncertain) and using Equations [39] and [40], the following values are derived

$$\eta_i = 0.808, \quad \eta_\epsilon = 0.841, \quad \eta = 0.679$$

From model tests, η has been determined as 0.656. Further, a value of 0.77 is obtained from these calculations for the ratio of the net thrust to the thrust at the rotor and a value of 0.725 from the model tests. These differences between calculations and test results may arise from the uncertainty of $(c_D)_S$ which probably is greater than assumed because of separation which arises from the shape of the shroud and from the pressure increase at the rotor.

6. INFLUENCE OF A FINITE NUMBER OF BLADES

The scheme which has been introduced for the action of the rotor has been chosen as simple as possible, viz., constant circulation along the lifting lines, a hub vortex of the combined strength of the lifting lines, and a system of vortices within the boundary of the rear jet. Furthermore, it has been assumed that the number of blades is infinite. In this section, the last assumption will not be made but the velocity components which are induced at a lifting line by n_R helical tip vortices together with a straight hub vortex of strength $(n_R \Gamma_R)$ will be considered.

Without going into details of the deduction (e.g., see Kawada[7]), it is stated that the ratio of both the tangential and axial velocity components at a lifting line for a finite number of blades to the respective quantity for an infinite number of blades is expressed by the following relation

$$\frac{w_t}{(w_t)_\infty} \quad \frac{w_a}{(w_a)_\infty} = 1 - \frac{2n_R}{\tan \beta_R} S$$

where

$$S = \sum_{m=1}^{\infty} m I_{mn_R}\left(\frac{x}{\tan \beta_R}\right) K'_{mn_R}\left(\frac{m n_R}{\tan \beta_R}\right)$$

Within these expressions, $\tan \beta_R$ is the pitch angle of the tip vortices, I and K are the modified Bessel functions of the first and second kind, respectively, and the prime indicates the derivative with respect to the argument. When varying the number of blades, it is assumed that both the total circulation $(n_R \Gamma_R)$ and the pitch angle β_R are kept constant. This implies that the loading coefficient varies when the number of blades is varied.

The sum S depends on the pitch angle β_R and on the number of blades n_R. For $n_R = 5$, the quantity i_t which is related to S by

$$i_t \quad \frac{1}{2} \quad \frac{\tan \beta_R}{n_R^2}$$

is represented on Figure 14. This quantity i_t is denoted as the "induction factor." Then, the ratio of the velocity components becomes in terms of the induction factor

$$\frac{w_t}{(w_t)_\infty} \quad \frac{w_a}{(w_a)_\infty} \quad 1 + \frac{i_t}{n_R} \frac{x}{1-x}$$

By the use of single tip vortices, the induced velocity components are exaggerated near the tip since, when $x = 1$, both w_t and w_a become infinite. Beyond a certain distance from the tip, however, this formula is suitable for obtaining an order of magnitude for the influence of a finite number of blades. For β_R 33 degrees, e.g., the right-hand side becomes 1.020 at $x = 0.6$, [illegible] but in the range of β_R occurring in practice, the influence of a finite number of blades [illegible] very important. This holds for the

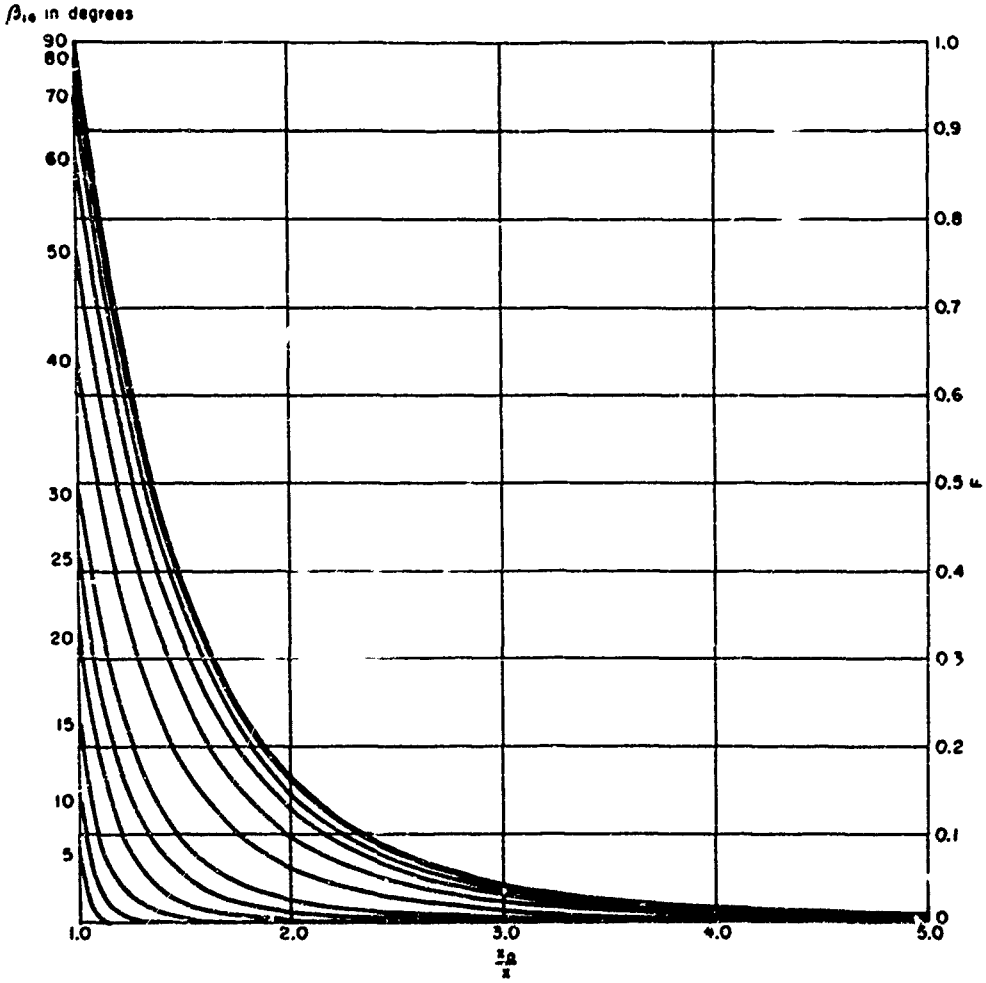

Figure 14

assumption that the circulation at the lifting lines is independent of the radius but is different when the circulation distribution depends on the number of blades (as it does with an unshrouded optimum propeller).

The same considerations are applicable for guide vanes with a finite number of blades. The influence of the number of blades on the induced velocity component is greater for the guide vanes than for the rotor since $\beta_V > \beta_R$. The induction factor increases when β increases, hence the factor is somewhat greater for the guide vanes than for the rotor. For $\beta_R = 33$ degrees and $\lambda = 0.45$, e.g., β_V becomes 56 degrees, with which quantity the correction to the velocity components from an infinite number of blades is 1.028 for $n_V = 6$ and $x = 0.6$. When the number of blades is increased, the percent correction decreases fairly rapidly, roughly to half its value when one blade is added (e.g., to 1.016 for $n_V = 7$).

7. METHOD OF DESIGN

The method of design of a shrouded unit from the foregoing considerations is analogous to that of the application of the usual propeller theory for design purposes.

The given quantities are loading coefficient c_T' (or c_p'), advance coefficient λ, pressure increase at the rotor p_R/p_0, and the cavitation number of the oncoming flow $\sigma_0 = (p_0 - p^*) / \frac{\rho}{2} v_0^2$ When a value of $h = l/2R$ is chosen, the circulation at the shroud, required, in order to realize the pressure increase becomes known from Equation [23b] and Figure 2.

$$G_S = \frac{1-\sqrt{1-\frac{\Delta p}{\frac{\rho}{2} v_0^2}}}{\left|\left(\frac{w_a}{v_0}\frac{1}{G}\right)_{D,S}\right|} \qquad [23b]$$

The quantity $\Delta p/(\rho/2)v_0^2$ is related to p_R/p_0 and σ_0 by

$$\frac{\Delta p}{\frac{\rho}{2} v_0^2} = \sigma_0 \left(\frac{p_R}{p_0} - 1\right)$$

The next step is to determine the loading coefficient of the system when operating in nonviscous flow; this requires the determination of the drag-lift coefficients of the components of the system. This problem can be solved by successive approximations when putting in a first step, $c_T' = c_T$ (with the power coefficient given, the method is entirely analogous). Then, the circulation at the rotor follows from Equation [24]

$$\left(\frac{n_R G_R}{\lambda}\right)^2 - \left(\frac{n_R G_R}{\lambda}\right) \pi \left(c_T - G_S F_2 + \frac{G_S^2 F_2^2}{2}\right) + c_T \frac{\pi^2}{4} (c_T - 2 G_S F_2) = 0,$$

F_2 is known from Figure 10 as a function of h.

Putting $c_T' = c_T$, a first approximation is obtained for $(n_R G_R)$ with which a first approximation for the sink density follows

$$\left|\frac{\bar{e_D}}{v_0}\right| = \sqrt{1 + \frac{2}{\pi}\frac{n_R G_R}{\lambda}} - 1 \qquad [22]$$

At this point, a check is made as to whether or not the quantity h chosen together with the given quantities are consistent with a cavitation-free flow on the shroud. The condition for this is that

$$\sigma_0 \geq \left(\frac{V}{v_0}\right)^2_{max} - 1 \qquad [34a]$$

where

$$\left(\frac{V}{v_0}\right)_{max} = \left(\frac{V_S}{v_0} + \frac{V_T}{v_0}\right)_{max}$$

and where

$$\left(\frac{V_S}{v_0}\right)^2 = \left[1 + G_S\left(\frac{w_a}{v_0}\frac{1}{G_S}\right)_{S,S} + \frac{1}{2\pi}\left|\frac{\overline{e_D}}{v_0}\right|\left(w_a \frac{2\pi}{\overline{e_D}}\right)_{S,D} + \frac{2}{\pi}\frac{G_S}{h}\sqrt{1-z^2}\cos\alpha\right]^2$$

$$+\left[G_S\left(\frac{w_r}{v_0}\frac{1}{G_S}\right)_{S,S} + \frac{1}{2\pi}\left|\frac{\overline{e_D}}{v_0}\right|\left(w_r \frac{2\pi}{\overline{e_D}}\right)_{S,D} - \frac{2}{\pi}\frac{G_S}{h}\sqrt{1-z^2}\sin\alpha\right]^2 \qquad [34]$$

(Relative to $(w_a)_{S,D}$, see the discussion on page 17 for positive values of z.)

In Equation [34a], the cavitation number of the oncoming flow σ_0 is a given quantity. Further, V_T/v_0 is known if a certain thickness form of the shroud is selected. Within Equation [34], G_S and $|\overline{e_D}|$ have already been determined and the velocity functions are known; see the table on page 30. In these first steps, the declination of the camber line α is assumed zero.

If the value of h selected does not satisfy Equation [34a], a greater length of the shroud, i.e., a greater h, is chosen and the calculations are repeated.

Assuming that the h satisfies the cavitation condition of Equation [34a], first approximations of the cavitation number on both the rotor and the guide vanes are obtained from

$$\sigma_R = \left(\frac{v_0}{V_R}\right)^2\left[\sigma_0 + \frac{\Delta p}{\rho/2 v_0^2} - \left(\frac{n_R G_R}{2\pi}\right)^2\left(\frac{1}{x^2} - 1\right)\right] \qquad [29]$$

and from

$$\sigma_V = \sigma_R\left(\frac{V_R}{v_0}\right)^2\left(\frac{v_0}{V_V}\right)^2 \qquad [32]$$

where

$$\left(\frac{V_R}{v_0}\right)^2 = \left[1 + \frac{1}{2}\left|\frac{\overline{e_D}}{v_0}\right| - G_S\left|\left(\frac{w_a}{v_0}\frac{1}{G_S}\right)_{D,S}\right|\right]^2 + \left[\frac{x}{\lambda} - \frac{n_R G_R}{2\pi x}\right]^2 \qquad [27]$$

and where

$$\left(\frac{V_V}{v_0}\right)^2 = \left[1 + \frac{1}{2}\left|\frac{\overline{e_D}}{v_0}\right| - G_S\left|\left(\frac{w_a}{v_0}\frac{1}{G_S}\right)_{D,S}\right|\right]^2 + \left(\frac{n_R G_R}{2\pi x}\right)^2 \qquad [30]$$

In these first approximations, both σ_R and σ_V are calculated only at the radius $x = 0.7$, which is sufficient for determining the drag-lift coefficients.

The maximum values of the lift coefficients which are permissible from the point of view of onset of cavitation on both the rotor and the guide vanes follow from these cavitation numbers together with diagrams on the critical cavitation number or on the minimum pressure of a family of suitable sections. In order to obtain approximations for the drag-lift coefficients, the drag coefficients $(c_D)_R$ and $(c_D)_V$ must be known for the type of sections chosen. A reasonable first assumption for the rotor is $c_D \doteq 0.008$. For the vanes, c_D is obtained as the sum of the frictional coefficient and the pressure drag coefficient, the latter depending on the angle of attack which is usually great at the vanes. At the shroud, the drag coefficient $(c_D)_S$ may be greater than the frictional coefficient, in spite of the shock-free flow, as a consequence of separation inside of the shroud which arises from its action as a diffusor and from the action of the rotor. No information on this effect could be found in the literature. Measurements on the drag coefficient of annular-shaped wings are restricted to accelerated flow, i.e., the nozzles. In this case and for a thickness ratio of the section of about 20 percent, a value of 0.015 for c_D at Reynolds number 4.10^5 has been determined. This figure is somewhat greater than would be expected for a two-dimensional wing of equal section.

The drag-lift coefficients of the components of the system being known approximately, the loading coefficient of the system in nonviscous flow c_T follows from

$$c_T = c_T' + (\epsilon_R + \epsilon_V)\frac{4}{\pi}\frac{n_R G_R}{1-x_h^2}\left[\left(1+\frac{1}{2}\left|\frac{\bar{e}_D}{v_0}\right|\right)(1-x_h) - G_S\int_{x_h}^{1}\left|\left(\frac{w_a}{v_0}\frac{1}{G_S}\right)_{D,S}\right|dx\right] + (c_D)_S\frac{4h}{1-x_h^2} \qquad [38]$$

The approximation is repeated in a second step with this value of c_T. Subsequent steps are necessary until the value of c_T which results in a certain step does not differ appreciably from that which was assumed for that step.

When c_T has been determined in this way, the exact values of G_S, G_R, $\bar{e}_D/v_0$, (V_R/v_0) and (V_V/v_0) can be ascertained, the last two quantities as functions of the radius x. Then the products $(c_L l)$ at both rotor and vanes follow as functions of x from

$$\frac{(c_L l)_R}{D} = 2\left(\frac{v_1}{V_1}\right)G_R \qquad [27]$$

and from

$$\frac{(c_L l)_V}{D} = 2\,\frac{n_R}{n_V}\left(\frac{v_0}{V_V}\right)G_R \qquad [30]$$

Further, at each radius, the cavitation numbers σ_R and σ_V become known from Equations [29] and [32], respectively. With the aid of the afore-mentioned diagrams for critical cavitation numbers of families of sections (which should include the two-dimensional cascade effect), the products $(c_L\, l)$ are so split up into their factors c_L and l that c_L equals or becomes smaller than that lift coefficient for the respective local cavitation number which is permissible relative to the onset of cavitation. With this lift coefficient, the angle of attack of the respective section against the resultant relative velocity is determined when the lift versus angle of attack curves of the sections, including the cascade effect, are known. The direction of the resultant relative velocity against the plane of the rotor is obtained for the rotor from

$$\tan \beta_R = \frac{1 + \frac{1}{2}\left|\frac{\bar{e}_D}{v_0}\right| - G_S\left|\left(\frac{w_a}{v_0}\frac{1}{G_S}\right)_{D,S}\right|}{\frac{x}{\lambda} - \frac{n_R G_R}{2\pi x}} \qquad [28]$$

and for the guide vanes from

$$\tan \beta_V = \frac{1 + \frac{1}{2}\left|\frac{\bar{e}_D}{v_0}\right| - G_S\left|\left(\frac{w_a}{v_0}\frac{1}{G_S}\right)_{D,S}\right|}{\frac{n_R G_R}{2\pi x}} \qquad [31]$$

The design of the shroud requires the integration of Equation [33] for the determination of the shape of the camber line and its orientation with respect to the axis. In this equation, all quantities are known from the preceding numerical calculations. The influence of axisymmetrical flow on the pressure distribution of the thickness form is approximately compensated for by an additional camber, from Figure 13, to be superimposed on the shape which follows from an integration of Equation [33]. At least two steps are necessary for determining the shape and the geometric angle of attack of the camber line from Equation [33], viz., arranging the vortices first on the rotor cylinder and, afterwards, on the camber line. Tables by Kuechemann in which the velocity components from both vortex and sink rings have been tabulated are very useful for the second and higher approximations.[8]

Finally, the efficiency of the system is obtained from Equations [39] and [40]. In the latter relation, the drag-lift ratios ϵ_R and ϵ_V are considered independent of r. In general, it will be sufficient to introduce the respective quantities at $x = 0.7$ as a suitable average.

8. CONCLUSION

The considerations of this paper are based on a circulation at the bound vortices of the rotor which is independent of the radius. This case represents the optimum with respect to efficiency for a shrouded propeller. The flow for circulation distributions which differ from the optimum can be determined in principle from the effects of the free vortex sheets

which are a consequence of a radially varying circulation and from their interference with the shroud vortices. Such problems arise when, e.g., a shrouded unit is given which satisfies the optimum circulation in the design condition and when the circulation distributions of both rotor and shroud are to be determined in an off-design condition. For a finite number of blades, this problem leads to an integral equation which can only be solved by approximate methods. The velocity field of vortex sheets with an arbitrary pitch distribution must be known in order to obtain a solution. The necessary numerical quantities of this velocity field have been ascertained at the lifting lines for a range of blade numbers. The determination of the induced velocities at the shroud, however, would require a great deal of additional numerical work

In addition to this theoretical work on units with a radially varying circulation, it is the opinion of the author that the following experimental work is necessary for a further development of shrouded propellers:

a. Studies of pressure distribution, separation, and radial distribution of the inside flow of annular-shaped wings whose flow is retarded. The available experimental papers[9,10] give information on pressure distribution, but no systematic information could be found either on the drag or on the velocity distribution of the inside flow. In addition, the influence of the shaft on the afore-mentioned quantities should be ascertained.

b. Studies on shrouded propellers with a transparent shroud are needed in order to investigate the cavitation performance of shroud, rotor, and guide vanes. Such investigations would be instructive both with regard to predictions from theory and to a judgment of the performance of the shrouded unit as a noise source in comparison with an unshrouded propeller.

9. REFERENCES

1. Dickmann, J., "Thrust Deduction, Wave Making Resistance of a Propeller and Interaction with Ship Waves," Ing. Archiv. 9, 1938.

2. Dickmann, J., "Fundamentals of the Theory of Annular-Shaped Wings," Ing. Archiv. 11, 1940.

3. Stewart, H.J., "The Aerodynamics of a Ring Airfoil," Quart. Appl. Math. 1, 1945.

4. Kuechemann, D., "Tables for the Stream-Function and the Velocity-Components of Source-Rings and Vortex-Rings," Jahrb. d. D.L., 1940.

5. Horn, W.F., "Design of Nozzle-Systems (Kort-Nozzles)," Jahrb. Schiffbaut. Ges., 1950.

6. Kuechemann, D., "Concerning the Flow about Ring Shaped Cowlings of Finite Thickness, Part 1," (Translation) NACA Tech Memo 1325, Jan 1952.

7. Kawada, S., "Induced Velocity by Helical Vortices," J. Aero. Sci. 3, 1936. See also, Report of the Aero. Res. Inst., Imp. Univ., Tokyo, 172, 1939.

8. Kuechemann, D. and Weber, J., "Further Measurements on Annular Profiles," (Translation) NACA Tech Memo 1328, Feb 1952.

9. Baals, D.D., "The Development and Application of High Critical Speed Nose Inlets," NACA Tech Rept 920, 1948.

10. Nichols, M.R., "Investigation of a Systematic Group of NACA 1-Series Cowlings with and without Spinners," NACA Tech Rept 950, 1949.

INITIAL DISTRIBUTION

Serials	
1-10	Chief, Bureau of Ships, Technical Library (Code 327), for distribution: 1-5 Code 327 6 Code 300 7 Code 420 8 Code 430 9 Code 436 10 Code 554
11-12	Chief, Bureau of Ordnance 11 Code Ad3 (Library) 12 Code Re6a
13-15	Chief, Bureau of Aeronautics 13 Code TD-42 (Library) 14 Code De-3 15 Code RS-7
16	Chief of Naval Operations, Department of Defense Building, Washington 25, D.C.
17	Chief of Naval Research, Attn: Mr. H.W. Lohley
18	Commander, U.S. Naval Ordnance Test Station, Pasadena Annex, 3202 E. Foothill Blvd., Pasadena 8, Calif.
19	Commander, U.S. Naval Ordnance Laboratory, White Oak, Silver Spring 19, Md.
20	Director, U.S. Naval Research Laboratory, Anacostia, Washington 20, D.C.
21	Director, U.S. Naval Engineering Experiment Station, Annapolis, Md.
22	Commander, U.S. Naval Air Development Center, Johnsville, Pa.
23	Superintendent, U.S. Naval Postgraduate School, Monterey, Calif.
24	Chairman, Research and Development Board, Department of Defense Building, Washington 25, D.C.
25	Secretary of the Air Force, Research and Development Division, Washington 25, D.C.
26	Commanding General, Wright-Patterson Air Force Base, Ohio, Office of Air Research
27	Commanding General, Langley Air Force Base, Va., Langley Aeronautical Laboratory, Attn: Mr. F.L. Thompson, Director of Research
28	Director, Technical Division, U.S. Maritime Administration, Washington 25, D.C.
29	Director of Aeronautical Research, National Advisory Committee for Aeronautics, 1724 F St. N.W., Washington 25, D.C.
30	Mr. John S. Coleman, Executive Secretary, National Research Council, Committee on Undersea Warfare, 2101 Constitution Ave., Washington 25, D.C.

Serials

31	Supervisor of Shipbuilding, USN, and Naval Inspector of Ordnance, New York, N.Y., for Gibbs and Cox, Inc., 21 West St., New York, N.Y. Attn: Mr. B.O. Smith
32	Inspector of Naval Material, Boston, Mass., forVADM E. L. Cochrane, Department of Naval Architecture and Marine Engineering, Massachusetts Institute of Technology, Cambridge 39, Mass.
33	Inspector of Naval Material, Los Angeles, Calif., for Hydrodynamics Laboratory, California Institute of Technology, Pasadena, Calif. Attn: Executive Committee
34	Inspector of Naval Material, 401 Water St., Baltimore 2, Md., for Dr. G.F. Wislicenus, Johns Hopkins University, Baltimore, Md.
35	Director, Office of Naval Research, Branch Office, Chicago, Ill., for Director, Iowa Institute of Hydraulic Research, State University of Iowa, Iowa City, Iowa
36	Director, Office of Naval Research, Branch Office, Chicago, Ill., for Director, St. Anthony Falls Hydraulic Laboratory, University of Minnesota, Minneapolis 14, Minn.
37	Director, Office of Naval Research, Branch Office, New York, N.Y., for Polytechnic Institute of Brooklyn, Department of Aeronautical Engineering and Applied Mechanics, Brooklyn, N.Y. Attn: Dr. H. Reissner
38	Development Contract Administrator, State College, Pa., for Pennsylvania State College, Ordnance Research Laboratory, State College, Pa. Attn: Dr. J.M. Robertson
39	Bureau of Aeronautics Representative, Inglewood, Los Angeles 45, Calif., for Propulsion Research Corporation, 309 E. Regent St., Inglewood 1, Calif. Attn: Mr. W.D. Crater
40	Bureau of Aeronautics Representative, Azusa, Calif., for Aerojet Engineering Corporation, Azusa, Calif. Attn: Dr. G.A. Gongwer
41	Bureau of Aeronautics Representative, c/o Bendix Aviation Corporation, Teterboro, N.J., for Stevens Institute of Technology, Experimental Towing Tank, 711 Hudson St., Hoboken, N.J. Attn: Dr. K.S.M. Davidson
42-50	British Joint Services Mission, P.O. Box 165, Benjamin Franklin Station, Washington, D.C.
51-53	Canadian Joint Staff (Navy), 1700 Massachusetts Ave. N.W., Washington, D.C.